DOI: 10.1002/chem.200800692

Synthesis and Conformational Analysis of Stevastelin C3 Analogues and Their Activity Against the Dual-Specific Vaccina H1-Related Phosphatase

Nicola Bisek,[a, b] Stefan Wetzel,[a, b] Hans-Dieter Arndt,*[a, b] and Herbert Waldmann*[a, b]

Abstract: The biological activity of macrocyclic natural products depends on their conformational properties. For both the elucidation of enzyme binding affinities as well as the development of selective drugs, rigid macrocyclic scaffolds carry high potential. In this study, 13-membered cyclodepsipeptides based on the structure of naturally occurring stevastelins were studied in detail. Six diastereomeric stevastelin C3 analogues and four phosphorylated derivatives were synthesized. The synthesis of linear precursors was achieved on solid support by starting from stereoisomerically pure 2-methyl-3-hydroxy acids. Subsequent macro-lactamization gave the cyclic depsipeptides in very good yields (36–62%). The conformational space of these stevastelin C3 analogues was computationally investigated. On the basis of NMR spectroscopic data, homogeneous conformations were determined for each benzylated depsipeptide and the influence of phosphorylation on the overall conformation was investigated. Importantly, phosphorylation was found to significantly weaken the conformational preferences of the 13-membered depsipeptides. Finally, the cyclic depsipeptides were tested for activity against phosphatases. Inhibitory activity on vaccina H1-related phosphatase was observed depending on the derivatization of the cycles. The activity profiles are discussed in the light of the structural data.

Keywords: biological activity · conformation analysis · cyclodepsipeptides · macrocyclization · phosphorylation

Introduction

Naturally occurring cyclic depsipeptides provide a rich source of structurally interesting compounds endowed with various biological activities. Prominent representatives even entered clinical trials. Among them kahalalide F (**1**)[1] has been shown to be a potent anticancer agent acting on cell lysosomes and is currently undergoing phase II clinical trials. Another relevant example is globomycin (**2**).[2] This cyclic lipodepsipeptide antibiotic leads to the accumulation of precursors of membrane lipoproteins in bacterial cell walls and thereby promotes cell death. In further biological studies, it has been found to be a specific inhibitor of lipoprotein signal peptidase II.[3]

However, within numerous cyclic depsipeptides only 39 13-membered rings can be found in the dictionary of natural products, representing seven different compound classes.[4] Lydiamycin A (**3**) has shown antibacterial activity against a series of mycobacteria, including *Mycobacterium tuberculosis*.[5] The beauveriolides I and III (**4, 5**) have an antiatherosclerotic effect in vivo and show promise as potential lead compounds for therapeutic agents.[6] Apart from antibacterial and antitumoral activities, some cyclic depsipeptides have shown immunosuppressive properties. Among them, the stevastelins (**6**–**12**; stevastelin A (**6**), B (**7**), A3 (**8**), B3 (**9**), C3 (**10**), D3 (**11**), E3 (**12**)) were identified, which have been isolated from a culture broth of *Penicillium*.[7] These depsipeptides have not only shown effects on the immune response but also inhibition of phosphatases.[8]

On the molecular level, cyclic peptides often display increased bioactivity and stability when compared to their linear epitopes.[9–11] Furthermore, cyclization of peptide chains has been used extensively as a method for introducing conformational constraints in peptide backbones and to

[a] Dipl.-Chem. N. Bisek, Dipl.-Chem. S. Wetzel, Dr. H.-D. Arndt, Prof. Dr. H. Waldmann
Abteilung Chemische Biologie
Max-Planck-Institut für Molekulare Physiologie
Otto-Hahn-Straße 11, 44227 Dortmund (Germany)
Fax: (+49) 231-133-2499
E-mail: hans-dieter.arndt@mpi-dortmund.mpg.de
herbert.waldmann@mpi-dortmund.mpg.de

[b] Dipl.-Chem. N. Bisek, Dipl.-Chem. S. Wetzel, Dr. H.-D. Arndt, Prof. Dr. H. Waldmann
Fakultät Chemie, Technische Universität Dortmund
Otto-Hahn-Straße 6, 44227 Dortmund (Germany)

Supporting information for this article is available on the WWW under http://dx.doi.org/10.1002/chem.200800692.

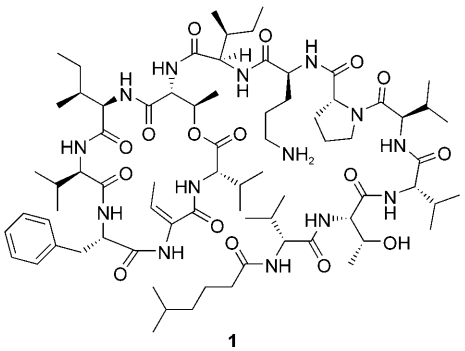

1

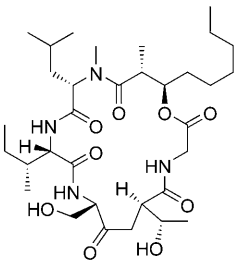

2

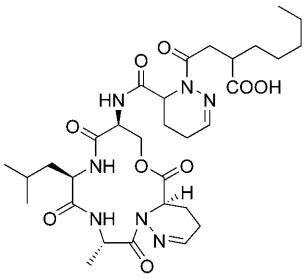

3

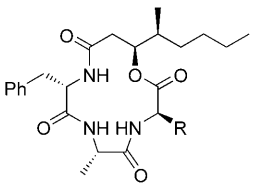

4: R = *i*Bu
5: R = *s*Bu

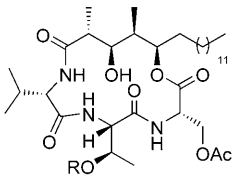

6: R = SO_3H
7: R = H

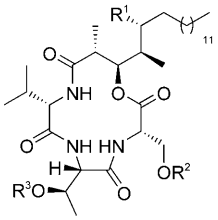

8: R^1 = OH, R^2 = Ac, R^3 = SO_3H
9: R^1 = OH, R^2 = Ac, R^3 = H
10: R^1 = H, R^2 = H, R^3 = H

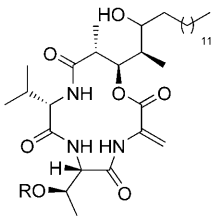

11: R = SO_3H
12: R = H

present diverse functionality in a defined and predictable manner.[12–14] Such conformational rigidification has not only been used for mimicking protein turns, but also for the design of orally available therapeutics.[15] Even slight changes in the macrocyclic backbone can influence biological activities dramatically.[16–18]

Therefore, a rigid macrocyclic scaffold for orientating potential enzyme binding groups in space would be highly valuable. Such a template could serve as powerful tool for the elucidation of enzyme binding affinities or the development of selective drugs, filling an enzyme pocket by arranging functional groups on the rigid template in a defined way.

In this regard, 13-membered cyclic depsipeptides are especially interesting as 12-membered tetrapeptides possess unfavorable ring strain resulting in instability and difficulties in synthesis, which often leads to the necessity for turn-inducing elements like prolines or D-amino acids.[19,20] Furthermore, many cyclic tetrapeptides show multiple conformations in water or DMSO.[21,22] Hence, the 13-membered cyclic depsipeptides characterized by one ester linkage belong to the smallest cyclic peptide scaffolds that can be accessed efficiently without the need of particular turn inducers.

Previously, it has been reported that different 13-membered stevastelin analogues display interesting biological activities on the dual-specific vaccina H1-related (VHR) phosphatase.[8,23] The inhibitory activity has been shown to depend on the configuration of the stereocenters in the β-hydroxy acid.

To systematically investigate the influence of stereochemical alterations in the backbone, we decided to develop a straightforward synthesis for a series of 13-membered stevastelin C3 analogues with variations of selected stereocenters in the backbone of the cyclic depsipeptide (**13**, **14**). Due to the strained macrocyclic system, we presumed low conformational flexibility. It was planned to compare the low-energy conformations of the diastereomeric macrocycles by using 2D NMR spectroscopic experiments and computational analysis of the conformational space and to investigate the influence of topological changes on the inhibitory activity against the dual-specific phosphatase VHR.

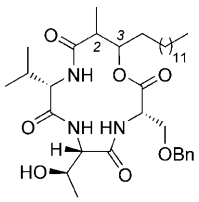

(2*R*,3*S*)-**13**
(2*R*,3*R*)-**13**
(2*S*,3*R*)-**13**
(2*S*,3*S*)-**13**

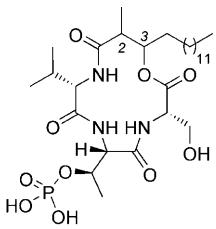

(2*R*,3*S*)-**14**
(2*R*,3*R*)-**14**
(2*S*,3*R*)-**14**
(2*S*,3*S*)-**14**

These results should lead to valuable insights into the potential of 13-membered cyclodepsipeptide scaffolds to serve the need for rigid templates for the elucidation of enzyme binding affinity and selectivity, in particular for phosphatase targeting.

Results and Discussion

Stevastelin C3 analogue synthesis: Our synthetic approach towards stevastelin C3 analogues (2*R*,3*S*)-**13**, (2*R*,3*R*)-**13**, (2*S*,3*R*)-**13**, and (2*S*,3*S*)-**13** involved solid-phase synthesis of the linear peptide esters **27** from building blocks **18**–**21** and the three amino acids, L-Ser, L-Thr, and L-Val. Subsequent macrolactamization in solution was planned to yield the cyclic depsipeptides (2*R*,3*S*)-**13**, (2*R*,3*R*)-**13**, (2*S*,3*R*)-**13**, and (2*S*,3*S*)-**13**.

To sample the stereocenters in the macrocyclic backbone, four different β-hydroxy acids were synthesized as outlined in Scheme 1. *anti*-Configured acids **18** and **20** were accessed

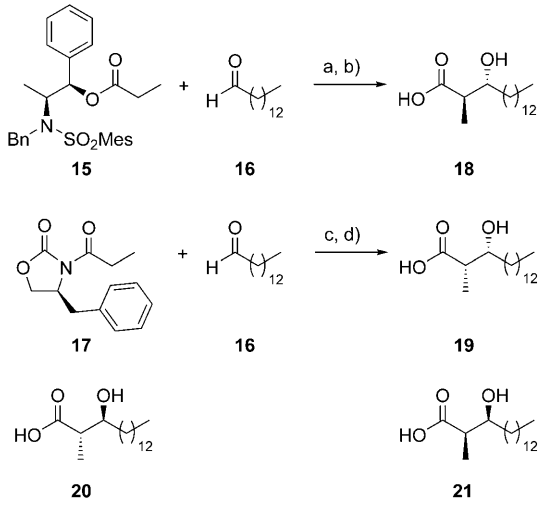

Scheme 1. Asymmetric synthesis of β-hydroxy acid building blocks: a) *c*Hex$_2$BOTf, NEt$_3$, CH$_2$Cl$_2$, −78 °C to RT, 3 h, d.r. 96:4, 71 %; b) 30 % H$_2$O$_2$, *n*Bu$_4$NOH, THF, 0 °C to RT, then Na$_2$SO$_3$, 86 %; c) *n*Bu$_2$BOTf, DIPEA, CH$_2$Cl$_2$, −78 °C to 0 °C, 2 h, d.r. 92:8, 80 %; d) 30 % H$_2$O$_2$, LiOH, THF/H$_2$O, 0 °C, 2 h then Na$_2$SO$_3$, 77 %. β-Hydroxy acids **20** and **21** have been synthesized accordingly by using the enantiomeric auxiliaries. DIPEA: diisopropyl ethyl amine. Tf: trifluoromethanesulfonyl.

by using the asymmetric aldol reaction developed by Abiko and Masamune,[24] whereas *syn*-configured acids **19** and **21** were prepared by using Evans aldol methodology.[25,26] The acylated auxiliaries **15** and **17** and their enantiomers were prepared by following known procedures.[27–29] Tetradecanal (**16**) was derived from its alcohol by oxidation with *o*-iodoxybenzoic acid (IBX).[30]

The *anti*-aldol products **18** and **20** were synthesized by adding tetradecanal **16** to the boron-enolate derived from norephedrin ester **15** or *ent*-**15** and *c*Hex$_2$BOTf and yielded the aldol adducts in a 71 % yield and with diastereomeric ratio of 96:4. After separation of the stereoisomers by column chromatography, the chiral auxiliary was cleaved by hydrolysis with aqueous *n*Bu$_4$NOH and H$_2$O$_2$ to give pure 2-methyl-3-hydroxy acids **18** and **20** in 86 % yield. For reproducible results, it was crucial to use freshly distilled aldehyde **16**.

The *syn*-aldol adducts were prepared in 80 % yield and with a diastereomeric ratio of 92:8. To this end, tetradecanal was added to the boron-enolate derived from Evans imides **17** or *ent*-**17** and *n*Bu$_2$BOTf in the presence of DIPEA. Cleavage of the auxiliary with aqueous LiOH and H$_2$O$_2$ yielded acids **19** and **21**, respectively.

For a flexible and straightforward synthesis, we focused on a solid-phase synthesis with a 2-chlorotrityl chloride resin (**22**) that tolerates the reaction conditions and can be cleaved in one step with Boc and *t*Bu protecting groups. The synthesis of linear depsipeptide (2*S*,3*R*)-**27** is exemplified in Scheme 2.

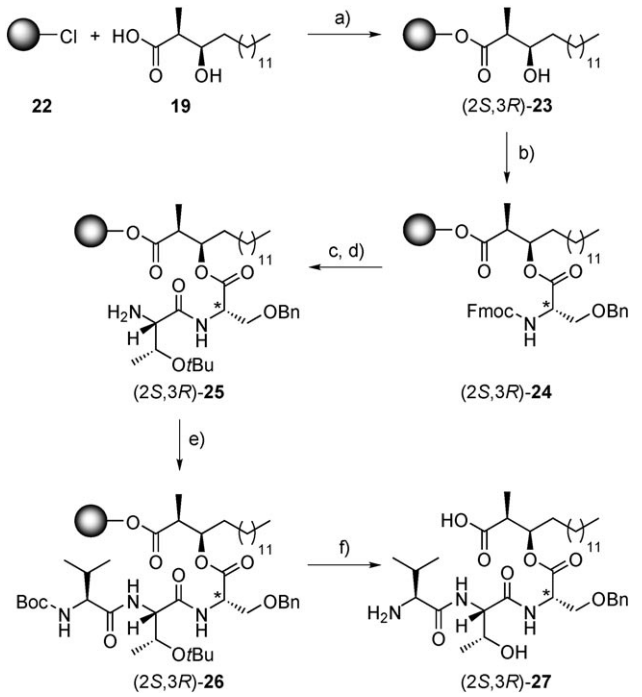

Scheme 2. Solid-phase synthesis of the linear cyclization precursors: a) DIPEA, CH$_2$Cl$_2$, 2.5 h, 99 %; b) FmocSer(OBn)OH, DIC, DMAP, CH$_2$Cl$_2$/DMF, 0 °C, 3 h, d.r. 8:1, 98 %; c) 2 × 15 min 20 % piperidine in DMF, 99 %; d) FmocThr(O*t*Bu)OH, DIC, HOBt, CH$_2$Cl$_2$/DMF, 2.5 h, 99 %; e) BocValOH, DIC, HOBt, CH$_2$Cl$_2$/DMF, 2.5 h, 99 %; f) 2 × 30 min TFA/CH$_2$Cl$_2$ (1:1), 88 % overall yield, d.r. 8:1. Boc: *tert*-butyloxycarbonyl; DIC:diisopropylcarbodiimide; DMAP: 4-dimethylaminopyridine; Fmoc: fluorenylmethyloxycarbonyl; HOBt: hydroxybenzotriazole; TFA: trifluoroacetic acid.

The hydroxy acid **19** was chemoselectively attached to resin **22** in the presence of DIPEA in CH$_2$Cl$_2$. Initial esterification attempts of FmocSer(OBn)OH and the immobilized β-hydroxy acid **23** showed epimerization of the serine in a ratio of 5:1. By lowering the temperature to 0 °C and the amount of DMAP to 0.2 equivalents, the reaction could be improved to a diastereomeric ratio of 8:1. Alternatively, Yamaguchi conditions[31] (2,4,6-trichlorobenzoyl chloride, NEt$_3$) could be applied, but delivered comparable yields and stereoisomeric purities.

The Fmoc group of resin-attached ester **24** was removed with 20% piperidine in DMF and subsequent coupling of FmocThr(O*t*Bu)OH with DIC and HOBt yielded immobilized depsipeptide **25**. Elongation of the sequence by Fmoc deprotection and coupling of BocValOH resulted in **26**. Finally, cleavage from the solid support with simultaneous deprotection of the Boc and *t*Bu groups with 50% TFA in CH_2Cl_2 released the desired cyclization precursor (2*S*,3*R*)-**27** together with its α-serine epimer. As separation of epimers at this point of synthesis proved to be difficult, the mixtures were cyclized and the isomers separated afterwards. The diastereomers ((2*R*,3*R*)-**27**, (2*R*,3*S*)-**27**, (2*S*,3*S*)-**27**) of the linear precursor were prepared in the same manner in excellent overall yields (80–90%).

The key step of our synthesis was the ring closure of the strained 13-membered depsipeptide. Macrolactamization of (2*S*,3*R*)-**27** with HBTU and DIPEA under high dilution conditions and separation of diastereomers by preparative HPLC afforded stevastelin C3 analogue (2*S*,3*R*)-**13** in 46% yield and epimer (2*S*,3*R*)-**30** in 7% yield (Scheme 3). The

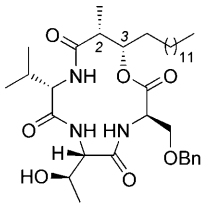
(2*R*,3*S*)-**30**

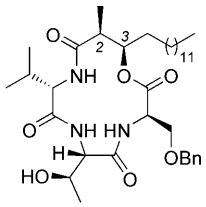
(2*S*,3*R*)-**30**

formation of cyclic dimers could be suppressed by slowly adding the open-chain precursor to a solution of coupling reagents with the help of a syringe pump. Following this strategy, three additional diastereomeric macrocycles ((2*R*,3*R*)-**13** in 36%, (2*S*,3*R*)-**13** in 55%, (2*S*,3*S*)-**13** in 62% yield) and two of the minor epimers could be isolated ((2*R*,3*S*)-**30** in 7%, (2*S*,3*R*)-**30** in 8% yield). Pd/C-catalyzed benzyl ether hydrogenolysis of cyclic depsipeptide (2*S*,3*R*)-**13** delivered stevastelin C3 analogue **29** in 77% yield.

Earlier studies had suggested that neutral stevastelins become phosphorylated or sulfated in vivo to reach their full activity.[8] Therefore, macrocycles (2*S*,3*R*)-**13**, (2*R*,3*R*)-**13**, (2*R*,3*S*)-**13**, and (2*S*,3*S*)-**13** were functionalized further (Scheme 3). Derivatization was achieved in three steps. Phosphitylation of the threonine residue in macrocycle (2*S*,3*R*)-**13** with *O,O*-dibenzyl(*N,N*-diisopropyl)phosphoramidite[32] and subsequent oxidation gave the phosphorylated macrocycle (2*S*,3*R*)-**28**. To avoid phosphonate formation, it was crucial to work under rigorously dry conditions. Furthermore, the very mild oxidation reagent *t*BuOOH was found to be optimal to suppress acid-mediated side reactions. Finally, macrocycle (2*S*,3*R*)-**28** was debenzylated quantitatively by Pd/C-catalyzed hydrogenolysis to give the phosphorylated analogue (2*S*,3*R*)-**14**. Diastereomeric analogues (2*R*,3*R*)-**14**, (2*R*,3*S*)-**14**, and (2*S*,3*S*)-**14** have been synthesized accordingly in excellent yields.

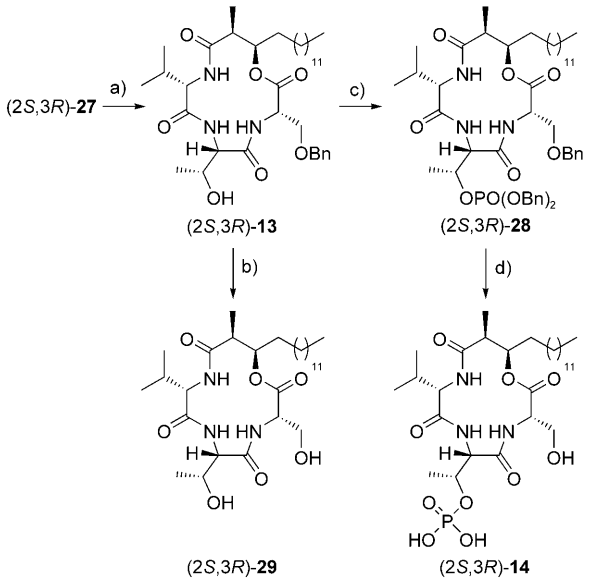

Scheme 3. Macrolactamization and derivatization of stevastelin C3 analogues: a) HBTU, DIPEA, CH_2Cl_2/DMF, 1.5 mM, RT, o/n, separation of diastereomers, 46% with L-Ser, 7% with D-Ser; b) 10% Pd/C, H_2, HCl, EtOH, o/n, 91%; c) tetrazole, $(BnO)_2PN(iPr)_2$, CH_2Cl_2, RT, then 0°C, *t*BuOOH, 77%; d) 10% Pd/C, H_2, EtOH, 4 h, 99%. HBTU: *o*-benzotriazol-1-yl-*N,N,N′,N′*-tetramethyluronium hexafluorophosphate; o/n: overnight.

In summary, a new straightforward synthesis of stevastelin C3 analogues has been developed. The esterification on solid support was found to be particularly challenging. The key steps towards stevastelin analogues **13** and **14** have been the macrolactamization of the linear depsipeptide and subsequent phosphorylation of the macrocycle. These reactions were optimized successfully to yield the analogues in very good yields. Due to the high yielding and flexible building-block approach, this synthesis needs only a few purification steps and can also be applied for the incorporation of other building blocks, such as modified β-amino acids, instead of the fatty acid or D-amino acids for further variation of the stereocenters in the peptidic backbone.

Conformational analysis: To investigate the ability of the diastereomeric macrocycles (2*S*,3*R*)-**13**, (2*R*,3*R*)-**13**, (2*R*,3*S*)-**13**, and (2*S*,3*S*)-**13** as well as D-serine-containing macrocycles (2*S*,3*R*)-**30** and (2*R*,3*S*)-**30** to serve as 3D templates for defined and predictable orientation of residues in space, these compounds were studied in detail.

In ^{1}H NMR spectroscopic experiments, a single set of resonances without line broadening was found for all molecules, which indicates just one stable conformation or fast averaging. Only macrocycle (2*R*,3*R*)-**13** showed line broadening for valine signals suggesting some intermediate flexibility at this position. TOCSY, gHSQC, and gHMBC experiments were then performed for complete signal assignment.

Comparison of ^{1}H NMR spectroscopic experiments of different stereoisomers in [D_6]DMSO already provided strong indications of different conformations, as dramatic differen-

ces in chemical shifts and coupling constants for both the CH^{α}- and NH-protons were observed. In proteins and linear peptides an upfield shift of NH and CH^{α} is known to correlate with helical structures, whereas a downfield shift is related to β-sheet conformations.[33] As the conformations of small and constrained peptide rings cannot be matched easily with proteins, one can only conclude that different stereoisomers induce distinct conformations within the macrocyclic ring. For instance, the comparison between the epimers (2*S*,3*R*)-**13** and (2*S*,3*S*)-**13** (Figure 1) demonstrates drastic differences in chemical shifts of Ser-NH and Thr-NH protons of $\Delta\delta = 0.79$ and 0.43 ppm, respectively. Furthermore, the α-protons and Val-H^{β} are significantly affected as well.

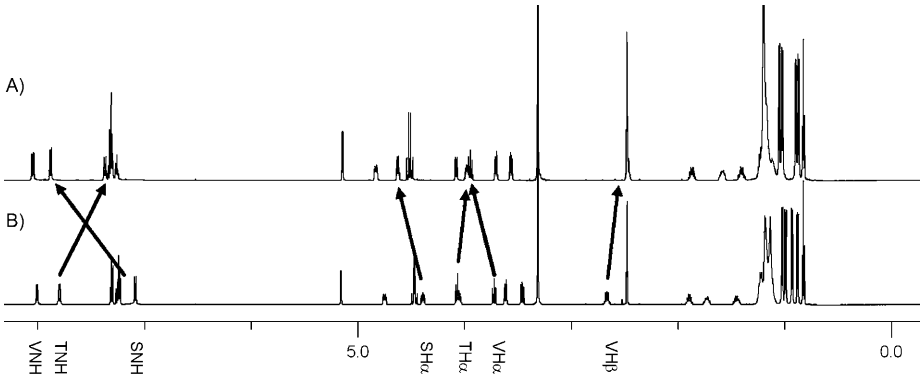

Figure 1. Comparison of ^{1}H NMR spectra in [D_6]DMSO of the two epimers of **13**. The spectra show significant shifts in the NH and CH^{α} region. A) (2*S*,3*R*)-**13**; B) (2*S*,3*S*)-**13**.

An all-*trans* peptide conformation was evident for all stereoisomers from NOE crosspeaks of NH protons and dihedral angle calculations from $^{3}J(NHCH^{\alpha})$ coupling constants (>8.2 Hz) by using the Karplus equation (Table 1).[34,35] Due to the significant differences in 1D NMR experiments when altering the stereocenters in the macrocyclic backbone, we were encouraged to investigate the conformations in more detail. Therefore, 2D ROESY experiments were performed and used to identify and quantify intramolecular proton–proton contacts. The calculated proton distances along the depsipeptide backbone and selected interresidual correlations are shown exemplarily for macrocycle (2*S*,3*R*)-**13** (Figure 2). 33 to 40 proton–proton distances have been assigned and qualified for each diastereomer. These distances were classified into approximately 24 interresidual, 12 sequential, and one medium-range contact. Only distinctly assigned protons have been used in further studies. Diastereotopic protons and torsion angles have been used for structure validations. More details can be found in the Supporting Information.

Table 1. Shifts and coupling constants of NH protons in [D_6]DMSO.

	SNH		TNH		VNH	
	δ [ppm]	*J* [Hz][a]	δ [ppm]	*J* [Hz][a]	δ [ppm]	*J* [Hz][a]
(2*S*,3*S*)-**13**	7.086	8.33	7.796	9.30	8.007	8.21
(2*R*,3*R*)-**13**	7.721	8.98	7.937	10.09	7.599	nd[b]
(2*S*,3*R*)-**13**	7.879	8.71	7.369	9.74	8.048	10.11
(2*R*,3*S*)-**13**	6.785	9.31	7.966	9.55	7.685	9.23
(2*S*,3*R*)-**30**	7.090	6.52	7.622	9.25	8.230	9.84
(2*R*,3*S*)-**30**	7.596	8.36	7.366	9.29	7.805	7.46

[a] $^{3}J(NHCH^{\alpha})$. [b] Not detected, one broad signal.

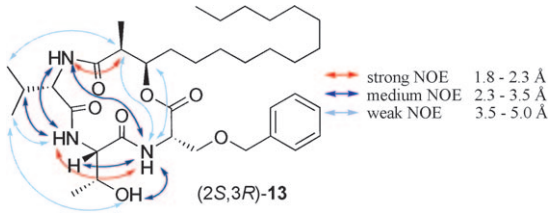

Figure 2. Selected ROESY contacts of macrocycle (2*S*,3*R*)-**13**.

Based on NMR-derived distance constraints, a conformational search was performed by using the low-mode search (LMOD) algorithm that has been especially developed for calculations of protein loops and cyclic peptides.[36] The low-energy conformations of the cyclic depsipeptides were computed with Macromodel 9.1[37] within Maestro. A total of 35,000 starting structures were generated, energy-minimized (OPLS2005, GB/SA solvation model), and compared.

By using the LMOD method and conformational energy calculations, we found stable low-energy structures for each analogue without dramatic violations of experimentally validated restraints (Figure 3). Comparing the diastereomeric stevastelin C3 analogues **13**, the lowest global energy could be found for (2*S*,3*S*)-**13** ($-258.3\ kJ\,mol^{-1}$) followed by the *syn*-configured analogues (2*S*,3*R*)-**13** and (2*R*,3*S*)-**13** (-239.4 and $-237.0\ kJ\,mol^{-1}$). Macrocycle (2*R*,3*R*)-**13** exhibited the highest global energy ($-229.3\ kJ\,mol^{-1}$) with a difference of $29\ kJ\,mol^{-1}$ relative to (2*S*,3*S*)-**13**.

In these calculated conformations, the orientation of the amino acid side chains is comparable for all the analogues, as they are all pointing to one side of the macrocycle. However, the long alkyl chain of the fatty acid can be oriented by setting the stereocenter in C-3 of the β-hydroxy acid.

In detail, we find that macrocyles (2*S*,3*S*)-**13** and (2*R*,3*S*)-**13** possess nearly identical backbone conformations. They only differ in the orientation of the methyl group at the altered stereocenter. From this result, we can conclude that the orientation of the methyl group does not change the topology of the rigid template that seems to be set by the peptidic section of the cycle and the *S* configuration at C-3 of the β-hydroxy acid.

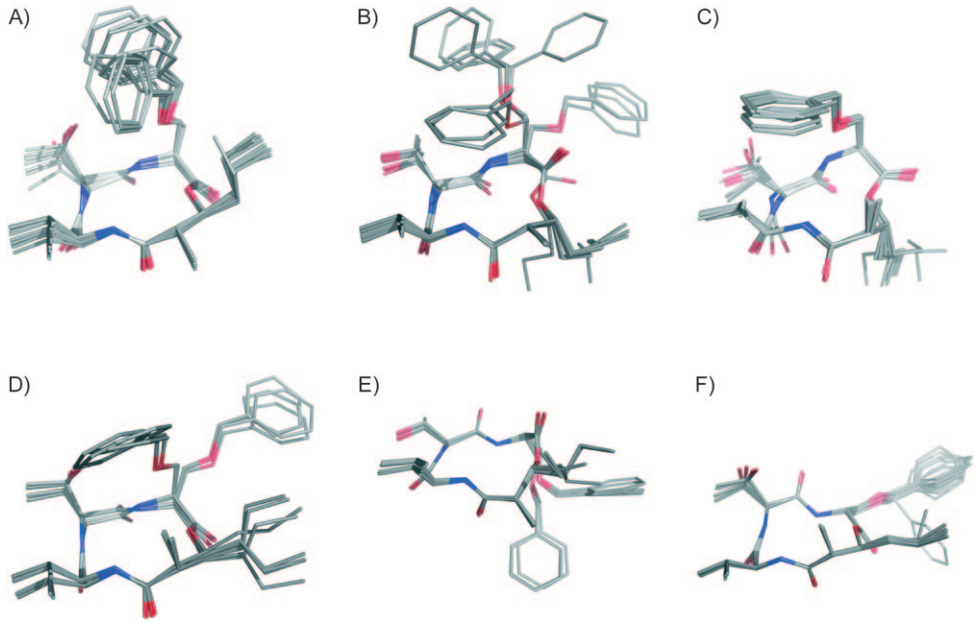

Figure 3. Ten lowest-energy conformations of stevastelin C3 analogues: A) (2*S*,3*S*)-**13**; B) (2*S*,3*R*)-**13**; C) (2*R*,3*R*)-**13**; D) (2*R*,3*S*)-**13**; E) D-Ser-containing (2*S*,3*R*)-**30**; F) D-Ser-containing (2*R*,3*S*)-**30**; grey = carbon, blue = nitrogen, red = oxygen.

In contrast to this result, macrocyles with an *R* configuration at C-3 behave completely differently. For diastereomers (2*R*,3*R*)-**13** and (2*S*,3*R*)-**13**, significantly different geometries of the backbone can be observed, which shows the strong influence of alteration in C-3 stereochemistry. Compound (2*R*,3*R*)-**13** has the same configuration as the natural stevastelin C3. Here, the *R* configuration of C-3 forces the macrocycle in a twisted form in which the threonine residue is bent downwards relative to backbone conformations of (2*S*,3*S*)-**13** and (2*R*,3*S*)-**13**, whereas the serine residue and carbonyl are bent upwards out of the plane of the cycle. In stevastelin analogue (2*S*,3*R*)-**13**, the *R* configuration of C-3 leads to an even more dramatic change in the orientation of the serine carbonyl, which is now pointing to the opposite side of the macrocyclic plane. In return, the threonine residue keeps the same geometry as in depsipeptides (2*S*,3*S*)-**13** and (2*R*,3*S*)-**13**.

Interestingly, an incorporated D-Ser did not lead to less-strained conformations as is known for cyclic tetrapeptides, but induced the opposite effect. Macrocycles (2*S*,3*R*)-**30** and (2*R*,3*S*)-**30** are energetically much less favored. Especially, analogue (2*S*,3*R*)-**30** ($-147.5\ kJ\,mol^{-1}$) is $92\ kJ\,mol^{-1}$ higher in energy than the its epimer (2*S*,3*R*)-**13** ($-239.4\ kJ\,mol^{-1}$). Besides the obvious effect on the orientation of the serine residue in cyclic analogues **30**, the valine carbonyl is pointing to the opposite side of the macrocycle relative to molecules **13**. In contrast to depsipeptide (2*S*,3*R*)-**13**, its epimer (2*S*,3*R*)-**30** shows completely different possibilities for the formation of hydrogen bonds and hydrophobic interactions.

Furthermore, the conformations of phosphorylated and debenzylated macrocycles **14** were analyzed. In a physiological surrounding phosphorylation is used as a key regulator of signal transduction by activation or deactivation of enzymatic functions. These effects are often caused by a change in protein conformation, due to the introduced steric hindrance, charge, and new possible hydrogen bonds after phosphorylation.[38–41] Normally, threonine phosphorylation leads to a coordination of the phosphate to the peptide backbone and thereby to a downfield shift of the coordinated NH.[42] However, comparing the synthesized macrocycles **13** and their phosphorylated and debenzylated analogues **14**, all amide protons are shifted downfield (Figure 4).

Additionally, phosphorylated macrocycles **14** show much broader signals in the ^1H NMR spectra than the benzylated cycles. As these findings can result from high flexibility in macrocycles **14**, a conformational search without constraints was performed and compared to unrestrained calculations of unphosphorylated macrocycles **13**. Indeed, it became evident that phosphorylation influences the backbone conformation and induces enormous flexibility. In an energy window of $50\ kJ\,mol^{-1}$ 147 conformation clusters (RMSD < $0.1\ kJ\,mol^{-1}$) can be found for phosphorylated cycle (2*S*,3*R*)-**14**, whereas only 14 clusters were found for unphosphorylated but benzylated cycle (2*S*,3*R*)-**13** (Table 2).

The phosphorylation-induced flexibility and signal broadening in the proton NMR can be explained by the calculated conformations of the phosphorylated cycles (Figure 5). In the strained macrocycle all amide protons are pointing towards the center of the cycle and the threonine residue places the phosphate just above the macrocyclic plane, which enables hydrogen bonding to any amide proton and the debenzylated serine residue.

In conclusion, we found conformationally homogeneous scaffolds for the benzylated molecules, which are determined by the stereocenters at C-2 and C-3 of the β-hydroxy acid part of the backbone and the α-Ser position. Altera-

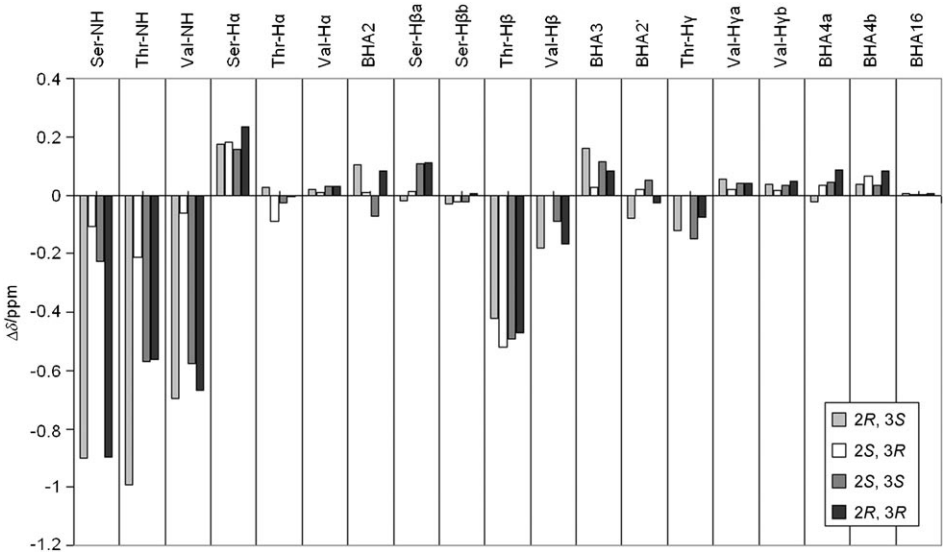

Figure 4. Differences in chemical shifts between unphosphorylated and phosphorylated macrocycles (**13**, **14**).

13-Membered cyclic tetrapeptides with incorporated β-amino acids instead of β-hydroxy acids have been shown to serve as rigid templates and are used as β- or γ-turn mimics.[14,43] But not all 13-membered peptides possess rigid conformations. It was reported, that the position of β-amino acid introduction is important to stabilize a single conformation.[14] Alternatively, 15-membered pentapeptides have frequently been used as conformationally rigid templates.[44–46] Furthermore, D-amino acids are known to induce βII′-turns[47,48] and the introduction of N-methylated amino acids lowers the energy barrier between *cis* and *trans* peptide bonds and leads to the loss of a hydrogen donor in the backbone generating new rigid templates.[12,48]

Application of such rigid scaffolds can be found in drug design. Kessler et al. have realized spatial screening with cyclic peptides, in which the conformation-inducing effect of special amino acids is utilized to generate rigid templates that are screened for their activity against selected enzymes.[13,49]

Hence, the synthesis of 13-membered depsipeptides serves as a new tool for the design of rigid macrocyles as biologically active compounds, which could be used to study

Table 2. Number of conformation clusters for each synthesized macrocycle within an energy window of 50 kJ mol^{-1}.

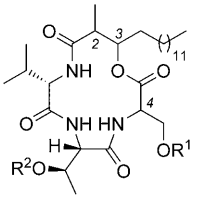

Inhibitor	Cluster[a]	Cluster[b]	R^1	R^2
(2*R*,3*S*)-**13**	32	2	Bn	H
(2*R*,3*R*)-**13**	37	21	Bn	H
(2*S*,3*R*)-**13**[c]	14	4	Bn	H
(2*S*,3*S*)-**13**	38	19	Bn	H
(2*R*,3*S*)-**14**	246	–	H	PO_3H_2
(2*R*,3*R*)-**14**	115	–	H	PO_3H_2
(2*S*,3*R*)-**14**	147	–	H	PO_3H_2
(2*S*,3*S*)-**14**	106	–	H	PO_3H_2

[a] Calculated without NMR-derived constraints. [b] Calculated with NMR-derived constraints. [c] Only 50% more unique structures were calculated for the debenzylated analogue (2*S*,3*R*)-**29**.

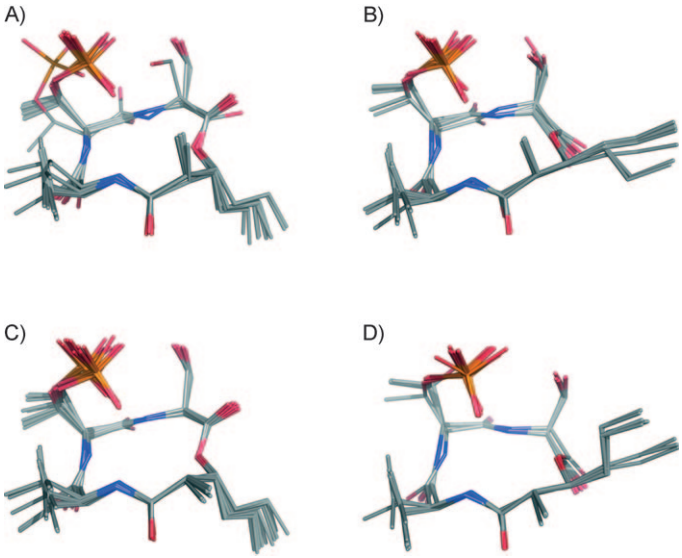

Figure 5. Low-energy conformations of phosphorylated stevastelin C3 analogues: A) (2*R*,3*R*)-**14**; B) (2*R*,3*S*)-**14**; C) (2*S*,3*R*)-**14**; D) (2*S*,3*S*)-**14**; grey = carbon, blue = nitrogen, red = oxygen, orange = phosphorus.

tions in these stereocenters do affect the macrocycle geometry. The orientation of the long alkyl chain seems to be more important than variation at C-2, which leads not only to different steric hindrance due to its orientation, but also populates a different conformation of the macrocyclic ring. In particular, the configuration at the α-Ser position determines the overall geometry of the stevastelin analogues, arranging possible enzyme binding groups in a completely different way. However, phosphorylation and subsequent debenzylation of the macrocyles leads to much more flexible structures, confirming the power of phosphorylation as a biological tool for switching conformational properties in peptides or proteins.

the affinity and selectivity of enzymes to give insights in their biological targets and functions.

Biochemical investigations: Due to the conclusive results from the conformational analysis in which different stable conformations for the synthesized stevastelin C3 analogues have been found, we were interested in the consequences on enzyme inhibition. As stevastelins have been reported to inhibit the dual-specific phosphatase VHR,[8] we investigated the inhibitory activity of the synthesized analogues against this phosphatase.

The 21 kDa dual-specific phosphatase VHR is one of the smallest known phosphatases.[50] It plays an essential role in MAP kinase regulation of cell cycle progression and the immune response in activated T-cells due to its activation by tyrosine kinase ZAP-70 and negative regulation of the mitogen-activated protein kinases, extracellular regulated kinases (ERK) and c-Jun N-terminal kinases (JNK).[51–53] To date, very few inhibitors of VHR are known.[8,54,55] New inhibitors or more detailed investigation of known inhibitors could give better insights into the physiological function of VHR and serve as lead structures for the development of new drug candidates.

VHR was assayed by using *para*-nitrophenol phosphate (*p*NPP) as a substrate. The reaction buffer contained 1 mM DTE to ensure an active state of the enzyme, as Cys-124 is involved in the catalytic enzyme mechanism.[56] Furthermore, 0.025% detergent NP-40 was found crucial to suppress unspecific binding. The assay was performed at an optimal pH of 6.5 and 37 °C.

Initially, the inhibitory activities of the synthesized compounds were tested at 100 μM. From active compounds, the IC_{50} values were determined. Only phosphorylated macrocycles inhibited the dual-specific phosphatase VHR in vitro, whereas unphosphorylated but benzylated stevastelin C3 analogues were inactive (Figure 6). Interestingly, only a slight dependence of inhibitory activity on orientation of the long alkyl chain could be observed (Table 3). An *S* configuration at position 2 of the β-hydroxy acid seems to be slightly favored, whereas an *R* configuration at position 3 gives better inhibition relative to its epimer.

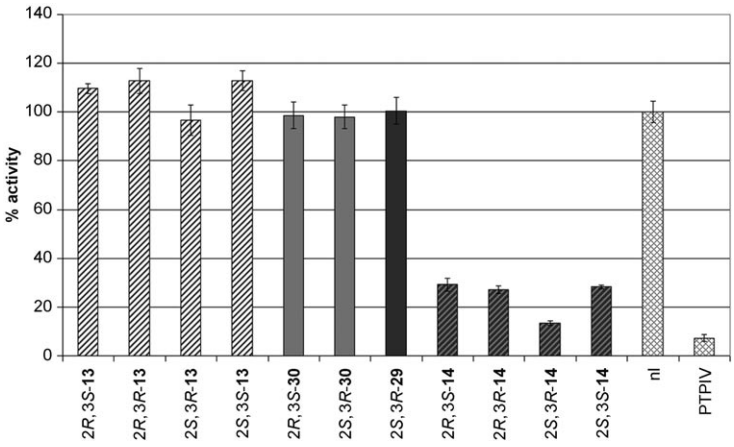

Figure 6. VHR inhibition at 100 μM inhibitor concentration. nI: control with no inhibitor; PTP inhibitor IV: control.

Table 3. Inhibition of dual-specific phosphatase VHR in vitro.

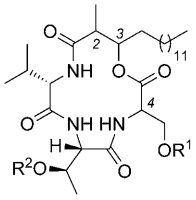

Inhibitor	IC_{50}(VHR)[b]	*2*[a]	*3*[a]	*4*[a]	R^1	R^2
(2*R*,3*S*)-**13**	>100 μM	*R*	*S*	*S*	Bn	H
(2*R*,3*R*)-**13**	>100 μM	*R*	*R*	*S*	Bn	H
(2*S*,3*R*)-**13**	>100 μM	*S*	*R*	*S*	Bn	H
(2*S*,3*S*)-**13**	>100 μM	*S*	*S*	*S*	Bn	H
(2*R*,3*S*)-**30**	>100 μM	*R*	*S*	*R*	Bn	H
(2*S*,3*R*)-**30**	>100 μM	*S*	*R*	*R*	Bn	H
(2*S*,3*R*)-**29**	>100 μM	*R*	*S*	*S*	H	H
(2*R*,3*S*)-**14**	(59.7±3.6) μM	*R*	*S*	*S*	H	PO_3H_2
(2*R*,3*R*)-**14**	(49.8±1.0) μM	*R*	*R*	*S*	H	PO_3H_2
(2*S*,3*R*)-**14**	(37.7±1.2) μM	*S*	*R*	*S*	H	PO_3H_2
(2*S*,3*S*)-**14**	(40.5±2.6) μM	*S*	*S*	*S*	H	PO_3H_2

[a] Configuration of the stereocenter. [b] Mean of three independent experiments.

These results stand in contrast to data reported earlier in the literature.[23] During the course of our studies, we found that VHR apparently seems to be very sensitive to changes in assay conditions, which makes these data difficult to compare. In the current investigations, a clear dependence on threonine derivatization has been found.

The minor differences in biochemical activity among the phosphorylated analogues (2*S*,3*R*)-**14**, (2*R*,3*R*)-**14**, (2*R*,3*S*)-**14**, and (2*S*,3*S*)-**14** are supported by our results from conformational analysis, in which these derivatives have shown higher flexibility than the unphosphorylated macrocycles. Furthermore, these new results support previous observations in which the natural stevastelins that are sulfated or phosphorylated are more active against VHR in vitro.[8] However, in living cells the reverse effect has been observed. Thus, the hypothesis was put forward that uncharged stevastelins penetrate the membrane and become phosphorylated or sulfated in the cell, thus generating the active form of the inhibitor in vivo. Our results suggest that this hypothesis may be valid for VHR. Recently, it has been shown, that VHR inhibition can lead to highly activated ERK and JNK resulting in a cell cycle arrest at the G1–S transition.[57] Therefore, further cellular studies of stevastelin C3 analogues **13** in HeLa cells are ongoing.

On the other hand, the phosphorylated stevastelin C3 analogues could also serve as substrates for the dual-specific phosphatase and become dephosphorylated. The natural substrate for VHR is a double phosphorylated protein, with phosphorylated Thr and Tyr separated by one amino acid in the peptide sequence.[58] It has been shown that VHR turns over phosphotyrosine very efficiently, whereas phosphothreonine and *p*NPP are converted rather slowly. To moni-

tor VHR-mediated phosphate release from the stevastelin analogues, a malachite green control experiment[59] was performed. The result shows that macrocyle (2*S*,3*S*)-**14** indeed serves as substrate, but gets dephosphorylated very slowly. After 45 min, 15% dephosphorylation could be observed.

Deactivation of the active inhibitor (2*S*,3*S*)-**14** by VHR-mediated dephosphorylation could, in principle, influence our assay results. However, in the performed setup the concentration of the substrate *p*NPP is much higher than the inhibitor concentration ((2*S*,3*S*)-**14**). Furthermore, with VHR a significantly higher $k_{cat.}/K_m$ was reported in the literature for *p*NPP in comparison to pThr,[58] which is present in (2*S*,3*S*)-**14**. Thus, from the equation for substrate specificity [Eq.: (1)], which describes the preferred enzymatic reaction in the presence of two potentially competing substrates, it follows that in our in vitro assay, competition should be negligible. Therefore, phosphorylated stevastelin analogues **14** are acting as inhibitors, not as substrates during our VHR assay, and IC_{50} values are not affected by dephosphorylation.

$$\frac{[v_I]}{[v_S]} = \frac{[k_{cat.}/K_m]_I[I]}{[k_{cat.}/K_m]_S[S]} \quad (1)$$

However, regarding their activity in cells, the phosphorylated stevastelins and analogues may become dephosphorylated by other endogeneous phosphatases. Therefore, either phosphorylation of the inhibitors must be competitive with phosphatase-mediated deactivation or the active molecule is not a phosphorylated stevastelin but another derivative, for example the sulfate.

Conclusion

Small macrocycles that are restrained in conformational flexibility can serve as 3D topological templates, which orientate potential enzyme binding groups in space. A series of 13-membered stevastelin C3 analogues was successfully synthesized based on solid-phase synthesis and macrocyclization in solution. Conformational studies on different stereoisomers revealed rigid conformations and defined orientation of functional groups attached to the macrocyclic backbone. Thus, we demonstrated that the introduction of a β-hydroxy acid into a small cyclic peptide can serve as a new tool for the generation of rigid macrocycles. These templates can be utilized for spatial screening against various enzymes to give insights into enzyme affinity and selectivity.

Furthermore, it could be shown that phosphorylation of the threonine moiety is essential for inhibitory activity against VHR in vitro. In phosphorylated and debenzylated analogues, the alteration of the backbone stereochemistry only moderately influenced the inhibitory activity on the dual-specific phosphatase VHR, which is in line with an increased level of flexibility of the cyclic depsipeptides after phosphorylation. As phosphorylated stevastelins were found to be substrates for VHR themselves, further biological studies are necessary to further explore the potential of the stevastelins as phosphatase inhibitors.

Experimental Section

General procedure: Immobilization of 2-methyl-3-hydroxyhexadecanoic acids: In a syringe reactor, 2-chlorotrityl chloride PS resin (1.4 mmol g^{-1}, 1.85 g, 2.59 mmol) was swollen in dry CH_2Cl_2 for 10 min before 2-methyl-3-hydroxytetradecanoic acid (965 mg, 3.37 mmol) and DIPEA (2.23 mL, 13.5 mmol) in dry CH_2Cl_2 (10 mL) were added. The mixture was shaken for 2.5 h at RT. Then the resin was washed with CH_2Cl_2 (3×), CH_2Cl_2/MeOH/DIPEA (17:2:1; 3×), CH_2Cl_2 (3×), MeOH (3×), and CH_2Cl_2 (3×) and dried in high vacuum overnight. A test cleavage with 5% TFA in CH_2Cl_2 showed quantitative loading.

General procedure: Esterification of the immobilized 2-methyl-3-hydroxyhexadecanoic acids: In a flask, 2-methyl-3-hydroxytetradecanoic acid (2.3 g, 2.4 mmol) loaded resin (**23**) was swollen in dry CH_2Cl_2 (10 mL) for 10 min. At 0°C, a solution of DIC (2.04 mL, 13.2 mmol) and FmocSer(OBn)OH (5.00 g, 12.0 mmol) in DMF/CH_2Cl_2 (1:1, 15 mL) was added, followed by DMAP (88 mg, 0.72 mmol) in DMF/CH_2Cl_2 (1:1, 5 mL) and the mixture was stirred at 0°C for 3 h. After washing the resin with CH_2Cl_2 (3×), DMF (3×), MeOH (3×), and CH_2Cl_2 (3×), the resin was dried at high vacuum overnight. An 86–96% yield was concluded from loading determinations. A test cleavage with TFA/CH_2Cl_2 (1:1) and subsequent HPLC analysis (chiral OD-H, 17% *i*PrOH in *n*hexane) showed a diastereomeric ratio of 89:11 to 82:18.

General procedure: Solid-phase peptide synthesis: For Fmoc deprotection, the resin was treated twice with 20% piperidine in DMF for 15 min each in a syringe reactor and washed with DMF and CH_2Cl_2. Then a solution of FmocThr(O*t*Bu)OH (5 equiv), HOBt (5 equiv), and DIC (5 equiv) in CH_2Cl_2/DMF (2:1) was added. The mixture was agitated for 3 h at RT and then washed with DMF, MeOH, and CH_2Cl_2 (3× each). The Fmoc deprotection and an amino acid coupling were repeated with BocValOH. Finally the resin was treated with TFA/CH_2Cl_2 (1:1) for 30 min twice. The resin was thoroughly washed with CH_2Cl_2 and the combined filtrates were coevaporated with toluene. After preparative HPLC, the product together with its Ser^{α}-epimer was obtained as a colorless solid. For the solid-phase synthesis of linear depsipeptides **27** an overall yield of 80–88% was calculated.

L-Valyl-L-threonyl-3-*O*-benzyl-L-seryl-(2*R*,3*S*)-2-methyl-3-hydroxyhexadecanoic acid ((2*R*,3*S*)-27): β-Hydroxy acid (2-methyl-3-hydroxyhexadecanoic acid) is represented as BHA throughout. Yield: 220 mg (331 μmol), 88% (d.r. 8:1); major isomer: ^{1}H NMR (400 MHz, $CDCl_3$): δ = 8.51 (d, J = 6.99 Hz, 1H; NH), 7.93 (d, J = 7.7 Hz, 1H; NH), 7.29–7.11 (m, 6H; aromat. H; NH), 5.26–5.19 (m, 1H; BHA3-H), 4.61–4.55 (m, 1H; Ser-H^{α}), 4.48 (d, J = 11.9 Hz, 1H; Ser-CH_2Ph), 4.44 (d, J = 11.9 Hz, 1H; Ser-CH_2Ph), 4.39 (d, J = 4.6 Hz, 1H; Thr-H^{α}), 4.07–3.97 (m, 1H; Thr-H^{β}), 3.90 (d, J = 6.0 Hz, 1H; Val-H^{α}), 3.82 (dd, J = 9.5, 4.1 Hz, 1H; Ser-H^{β}a), 3.65 (dd, J = 9.2, 3.2 Hz, 1H; Ser-H^{β}b), 2.59 (dq, J = 6.9, 2.6 Hz, 1H; BHA2-H), 2.15 (qd, J = 13.5, 6.8 Hz, 1H; Val-H^{β}), 1.60–1.47 (m, 1H; BHA4a-H_2), 1.45–1.33 (m, 1H; BHA4b-H_2), 1.26–1.09 (m, 23H; BHA), 1.13 (d, J = 6.3 Hz, 3H; Thr-H^{γ}), 1.09 (d, J = 7.1 Hz, 3H; BHA2′-H_3), 0.95 (d, J = 6.8 Hz, 6H; Val-H^{γ}), 0.86 ppm (t, J = 6.9 Hz, 3H; BHA16-H_3); ^{13}C NMR (101 MHz, $CDCl_3$): δ = 177.3 (BHA-1), 170.5 (Thr-1), 169.9 (Ser-1), 169.6 (Val-1), 137.1 (aromat. C), 128.3 (aromat. C), 127.8 (aromat. C), 127.6 (aromat. C), 75.9 (BHA-3), 73.4 (Ser-CH_2Ph), 69.0 (Ser-β), 67.2 (Thr-β), 59.4 (Thr-α), 58.7 (Val-α), 52.8 (Ser-α), 42.3 (BHA-2), 31.9 (BHA), 31.7 (BHA), 30.2 (Val-β), 29.7 (BHA), 29.6 (BHA), 29.4 (BHA), 29.3 (BHA), 25.5 (BHA), 22.6 (BHA), 18.8 (Thr-γ), 18.1 (Val-γa), 17.3 (Val-γb), 14.0 (BHA-16), 9.9 ppm (BHA-2′); IR (neat): $\tilde{\nu}$ = 3306, 3072, 2921, 2853, 1740, 1666, 1639, 1537, 1467 cm^{-1}; HPLC-ESIMS (C4–10; t_R = 8.32 min): m/z: 664.19 $[M+H]^+$, 1326.84 $[2M+H]^+$; HRMS (ESI): m/z: calcd for $C_{36}H_{62}N_3O_8$: 664.4531 $[M+H]^+$; found: 664.4528.

L-Valyl-L-threonyl-3-*O*-benzyl-L-seryl-(2*S*,3*R*)-2-methyl-3-hydroxyhexadecanoic acid ((2*S*,3*R*)-27): Yield: 267 mg (402 μmol), 87% (d.r. 8:1); major isomer: ^{1}H NMR (400 MHz, $CDCl_3$/MeOD 4:1): δ = 8.13 (d, J =

8.2 Hz, 1H; NH), 7.73 (d, J=8.2 Hz, 1H; NH), 7.24–7.09 (m, 5H; aromat. H), 5.12 (td, J=8.34, 4.96 Hz, 1H; BHA3-H), 4.55 (t, J=3.5 Hz, 1H; Ser-H$^{\alpha}$), 4.38 (s, 2H; Ser-CH_2Ph), 4.34 (d, J=4.6 Hz, 1H; Thr-H$^{\alpha}$), 4.01 (dq, J=6.4, 4.6 Hz, 1H; Thr-H$^{\beta}$), 3.79 (dd, J=9.6, 3.7 Hz, 1H; Ser-H$^{\beta}$a), 3.66 (d, J=6.1 Hz, 1H; Val-H$^{\alpha}$), 3.57 (dd, J=9.6, 3.4 Hz, 1H; Ser-H$^{\beta}$b), 2.52 (dq, J=7.0, 5.2 Hz, 1H; BHA2-H), 2.05 (qd, J=13.6, 6.9 Hz, 1H; Val-H$^{\beta}$), 1.56–1.35 (m, 2H; BHA4-H_2), 1.23–1.11 (m, 22H; BHA), 1.11 (d, J=6.5 Hz, 3H; Thr-H$^{\gamma}$), 1.03 (d, J=7.1 Hz, 3H; BHA2′-H_3), 0.89 (d, J=6.9 Hz, 3H; Val-H$^{\gamma}$a), 0.88 (d, J=6.9 Hz, 3H; Val-H$^{\gamma}$b), 0.75 ppm (t, J=6.9 Hz, 3H; BHA16-H_3); ^{13}C NMR (101 MHz, $CDCl_3$): δ=175.9 (BHA-1), 169.9 (Thr-1), 169.4 (Ser-1), 168.4 (Val-1), 137.0 (aromat. C), 128.2 (aromat. C), 127.7 (aromat. C), 127.4 (aromat. C), 75.9 (BHA-3), 73.2 (Ser-CH_2Ph), 69.2 (Ser-β), 67.2 (Thr-β), 58.4 (Thr-α), 58.3 (Val-α), 52.6 (Ser-α), 42.6 (BHA-2), 31.7 (BHA-4), 30.0 (Val-β), 29.4 (BHA), 29.2 (BHA), 29.1 (BHA), 25.1 (BHA), 22.4 (BHA), 18.3 (Thr-γ), 17.9 (Val-γa), 17.2 (Val-γb), 13.7 (BHA-16), 11.3 ppm (BHA-2′); IR (neat): $\tilde{\nu}$= 3292, 3066, 2922, 2852, 1740, 1688, 1666, 1658, 1641, 1544, 1536, 1468, 1454 cm^{-1}; HPLC-ESIMS (C4–10; t_R=8.39 min): m/z: 664.13 $[M+H]^+$, 1326.84 $[2M+H]^+$; HRMS (ESI): m/z: calcd for $C_{36}H_{62}N_3O_8$: 664.4531 $[M+H]^+$; found: 664.4528.

L-Valyl-L-threonyl-3-*O*-benzyl-L-seryl-(2*S*,3*S*)-2-methyl-3-hydroxyhexadecanoic acid ((2*S*,3*S*)-27): Yield: 252 mg (380 μmol), 80% (d.r. 8:1); major isomer: ^{1}H NMR (400 MHz, $CDCl_3$): δ=7.24–7.07 (m, 5H; aromat. H), 5.07–4.97 (m, 1H; BHA3-H), 4.57 (t, J=3.3 Hz, 1H; Ser-H$^{\alpha}$), 4.40–4.36 (m, 2H; Ser-CH_2Ph), 4.31 (d, J=4.5 Hz, 1H; Thr-H$^{\alpha}$), 4.07–3.98 (m, 1H; Thr-H$^{\beta}$), 3.79 (dd, J=9.5, 3.6 Hz, 1H; Ser-H$^{\beta}$a), 3.67 (dd, J=10.1, 6.0 Hz, 1H; Val-H$^{\alpha}$), 3.56 (dd, J=9.5, 3.3 Hz, 1H; Ser-H$^{\beta}$b), 2.66–2.55 (m, 1H; BHA2-H), 2.11–1.97 (m, 1H; Val-H$^{\beta}$), 1.53–1.41 (m, 2H; BHA-4), 1.21–1.07 (m, 22H; BHA), 1.05 (d, J=6.5 Hz, 3H; Thr-H$^{\gamma}$), 1.03–0.97 (m, 3H; BHA2′-H_3), 0.91–0.84 (m, 6H; Val-γ), 0.75 ppm (t, J=6.9 Hz, 3H; BHA16-H_3); ^{13}C NMR (101 MHz, $CDCl_3$): δ=175.5 (BHA-1), 169.7 (Thr-1), 168.7 (Ser-1), 168.4 (Val-1), 136.9 (aromat. C), 128.1 (aromat. C), 127.6 (aromat. C), 127.3 (aromat. C), 76.6 (BHA-3), 73.1 (Ser-CH_2Ph), 69.3 (Ser-β), 66.9 (Thr-β), 58.6 (Thr-α), 58.3 (Val-α), 52.6 (Ser-α), 42.7 (BHA-2), 31.6 (BHA), 31.0 (BHA), 30.8 (BHA), 30.0 (Val-β), 29.4 (BHA), 29.2 (BHA), 29.1 (BHA), 24.9 (BHA), 24.7 (BHA), 22.4 (BHA), 18.3 (Thr-γ), 17.9 (Val-γa), 17.0 (Val-γb), 13.7 (BHA-16), 12.7 ppm (BHA-2′); IR (neat): $\tilde{\nu}$=3277, 3066, 2924, 2853, 1742, 1659, 1525, 1465 cm^{-1}; HPLC-ESIMS (C4–10; t_R=8.44 min): m/z: 664.15 $[M+H]^+$, 1326.89 $[2M+H]^+$; HRMS (ESI): m/z: calcd for $C_{36}H_{62}N_3O_8$: 664.4531 $[M+H]^+$; found: 664.4528.

L-Valyl-L-threonyl-3-*O*-benzyl-L-seryl-(2*R*,3*R*)-2-methyl-3-hydroxyhexadecanoic acid ((2*R*,3*R*)-27): Yield: 133 mg (200 μmol), 82% (d.r. 8:1); major isomer: ^{1}H NMR (400 MHz, $CDCl_3$): δ=7.24–7.06 (m, 5H; aromat. H), 5.05–4.97 (m, 1H; BHA3-H), 4.51 (t, J=3.5 Hz, 1H; Ser-H$^{\alpha}$), 4.35 (s, 2H; Ser-CH_2Ph), 4.34–4.29 (m, 1H; Thr-H$^{\alpha}$), 4.04–3.95 (m, 1H; Thr-H$^{\beta}$), 3.77 (dd, J=9.6, 3.7 Hz, 1H; Ser-H$^{\beta}$a), 3.65 (d, J=5.9 Hz, 1H; Val-H$^{\alpha}$), 3.54 (dd, J=9.6, 3.4 Hz, 1H; Ser-H$^{\beta}$b), 2.64–2.52 (m, 1H; BHA2-H), 2.02 (qd, J=13.6, 6.9 Hz, 1H; Val-H$^{\beta}$), 1.52–1.37 (m, 2H; BHA-4), 1.18–1.03 (m, 25H; BHA, Thr-γ), 1.00 (d, J=7.1 Hz, 3H; BHA2′-H_3), 0.88–0.82 (m, 6H; Val-γ), 0.72 ppm (t, J=6.9 Hz, 3H; BHA16-H_3); ^{13}C NMR (101 MHz, $CDCl_3$): δ=175.9 (BHA-1), 169.9 (Thr-1), 169.2 (Ser-1), 168.4 (Val-1), 136.9 (aromat. C), 128.1 (aromat. C), 127.5 (aromat. C), 127.2 (aromat. C), 76.4 (BHA-3), 73.1 (Ser-CH_2Ph), 69.2 (Ser-β), 67.2 (Thr-β), 58.3 (Thr-α), 58.2 (Val-α), 52.6 (Ser-α), 42.9 (BHA-2), 31.6 (BHA), 30.8 (BHA), 29.9 (Val-β), 29.3 (BHA), 29.2 (BHA), 29.0 (BHA), 24.6 (BHA), 22.3 (BHA), 18.3 (Thr-γ), 17.8 (Val-γa), 17.0 (Val-γb), 13.6 (BHA-16), 12.5 ppm (BHA-2′); IR (neat): $\tilde{\nu}$= 3291, 3066, 2923, 2853, 1735, 1652, 1533, 1465 cm^{-1}; HPLC-ESIMS (C4–10; t_R=8.46 min): m/z: 664.16 $[M+H]^+$, 1326.71 $[2M+H]^+$; HRMS (ESI): m/z: calcd for $C_{36}H_{62}N_3O_8$: 664.4531 $[M+H]^+$; found: 664.4529.

General procedure: Macrolactamization: A solution of open chain precursor **27** (119 mg, 0.180 mmol) in dry CH_2Cl_2/DMF (15:1, 4 mL) was added slowly with a syringe pump to a solution of HBTU (137 mg, 0.360 mmol) and DIPEA (59 μL, 0.360 mmol) in dry CH_2Cl_2/DMF (15:1, 124 mL). The mixture was stirred for 14 h. After removal of the solvents, the residue was dissolved in ethyl acetate and washed with water and brine. The organic layer was dried with $MgSO_4$ and the ethyl acetate was removed. The crude product was purified by preparative HPLC, which provided both the title compound **13** and the minor epimer **30** resulting from partial epimerization of Ser-α as colorless powders.

1,3,4-Anhydro[L-valyl-L-threonyl-3-*O*-benzyl-L-seryl-(2*R*,3*S*)-2-methyl-3-hydroxyhexadecanoic acid] ((2*R*,3*S*)-13): Yield: 53.5 mg (82.8 μmol), 46%; $[\alpha]_D^{20}$=−45.9 (c=1 in $CHCl_3$); m.p.: 197°C; ^{1}H NMR (600 MHz, [D$_6$]DMSO): δ=7.97 (d, J=9.6 Hz, 1H; Thr-NH), 7.68 (d, J=9.2 Hz, 1H; Val-NH), 7.35–7.24 (m, 5H; aromat. H), 6.78 (d, J=9.3 Hz, 1H; Ser-NH), 5.28 (d, J=4.4 Hz, 1H; Thr-OH), 4.88 (ddd, J=8.4, 5.9, 2.3 Hz, 1H; BHA3-H), 4.55 (d, J=12.2 Hz, 1H; Ser-CH_2Ph), 4.47 (dt, J=9.1, 5.4 Hz, 1H; Ser-H$^{\alpha}$), 4.43 (d, J=12.2 Hz, 1H; Ser-CH_2Ph), 4.12–4.07 (m, 1H; Thr-H$^{\beta}$), 4.05 (dd, J=9.6, 2.4 Hz, 1H; Thr-H$^{\alpha}$), 3.86 (dd, J=11.1, 9.3 Hz, 1H; Val-H$^{\alpha}$), 3.52 (dd, J=9.2, 5.4 Hz, 1H; Ser-H$^{\beta}$a), 3.47 (dd, J= 9.1, 9.1 Hz, 1H; Ser-H$^{\beta}$b), 2.57 (dq, J=7.2, 2.1 Hz, 1H; BHA2-H), 2.03–1.95 (m, 1H; Val-H$^{\beta}$), 1.71–1.62 (m, 1H; BHA4a-H_2), 1.47–1.38 (m, 1H; BHA4b-H_2), 1.26–1.19 (m, 22H; BHA5–15-H_2), 1.17 (d, J=7.3 Hz, 3H; BHA2′-H_3), 1.02 (d, J=6.3 Hz, 3H; Thr-H$^{\gamma}$), 0.89 (d, J=6.5 Hz, 3H; Val-H$^{\gamma}$a), 0.87 (d, J=6.7 Hz, 3H; Val-H$^{\gamma}$b), 0.83 ppm (t, J=7.0 Hz, 3H; BHA16-H_3); ^{13}C NMR (151 MHz, [D$_6$]DMSO): δ=171.8 (BHA-1), 171.2 (Val-1), 170.2 (Thr-1), 167.4 (Ser-1), 137.6 (aromat. C), 128.1 (aromat. C), 127.5 (aromat. C), 127.4 (aromat. C), 76.4 (BHA-3), 72.1 (Ser-CH_2Ph), 68.8 (Ser-β), 64.8 (Thr-β), 62.0 (Val-α), 59.0 (Thr-α), 53.0 (Ser-α), 42.8 (BHA-2), 31.2 (BHA), 30.1 (BHA), 29.0 (Val-β), 28.9 (BHA), 28.7 (BHA), 28.6 (BHA), 24.5 (BHA), 22.0 (BHA), 20.7 (Thr-γ), 19.3 (Val-γa), 19.0 (Val-γb), 13.9 (BHA-16), 8.3 ppm (BHA-2′); IR (neat): $\tilde{\nu}$= 3424, 3283, 2923, 2853, 1745, 1671, 1656, 1536, 1468 cm^{-1}; HPLC-ESIMS (C4–70; t_R=5.13 min): m/z: 646.3 $[M+H]^+$, 668.5 $[M+Na]^+$; HRMS (ESI): m/z: calcd for $C_{36}H_{60}N_3O_7$: 646.4426 $[M+H]^+$; found: 646.4426.

1,3,4-Anhydro[L-valyl-L-threonyl-3-*O*-benzyl-D-seryl-(2*R*,3*S*)-2-methyl-3-hydroxyhexadecanoic acid] ((2*R*,3*S*)-30): Yield: 8.1 mg (12.6 μmol), 7%; m.p.: 178°C; ^{1}H NMR (600 MHz, [D$_6$]DMSO): δ=7.81 (d, J=7.5 Hz, 1H; Val-NH), 7.60 (d, J=8.4 Hz, 1H; Ser-NH), 7.37 (d, J=9.3 Hz, 1H; Thr-NH), 7.33–7.21 (m, 5H; aromat. H), 5.19 (dt, J=7.3, 2.4 Hz, 1H; BHA3-H), 4.78 (d, J=4.5 Hz, 1H; Thr-OH), 4.52 (ddd, J=8.1, 7.1, 5.4 Hz, 1H; Ser-H$^{\alpha}$), 4.48–4.42 (m, 2H; Ser-CH_2Ph), 4.11–4.04 (m, 2H; Thr-H$^{\beta}$, Thr-H$^{\alpha}$), 3.73 (dd, J=9.8, 7.5 Hz, 1H; Val-H$^{\alpha}$), 3.68 (dd, J=9.7, 7.1 Hz, 1H; Ser-H$^{\beta}$a), 3.50 (dd, J=9.7, 5.3 Hz, 1H; Ser-H$^{\beta}$b), 2.55 (dq, J=7.2, 2.3 Hz, 1H; BHA2-H), 2.18–2.08 (m, 1H; Val-H$^{\beta}$), 1.64 (qd, J= 14.0, 7.0 Hz, 1H; BHA4a-H_2), 1.48–1.40 (m, 1H; BHA4b-H_2), 1.26–1.19 (m, 22H; BHA5–15-H_2), 1.18 (d, J=7.3 Hz, 3H; BHA2′-H_3), 0.98 (d, J= 6.1 Hz, 3H; Thr-H$^{\gamma}$), 0.90 (d, J=3.3 Hz, 3H; Val-H$^{\gamma}$a), 0.88 (d, J=3.4 Hz, 3H; Val-H$^{\gamma}$b), 0.83 ppm (t, J=7.0 Hz, 3H; BHA16-H_3); ^{13}C NMR (151 MHz, [D$_6$]DMSO): δ=173.3 (BHA-1), 171.8 (Val-1), 169.8 (Thr-1), 169.0 (Ser-1), 138.2 (aromat. H), 128.1 (aromat. H), 127.2 (aromat. H), 75.8 (BHA-3), 72.1 (Ser-CH_2Ph), 67.5 (Ser-β), 64.3 (Thr-β), 62.9 (Val-α), 57.0 (Thr-α), 51.0 (Ser-α), 41.6 (BHA-2), 31.2 (BHA), 30.4 (BHA), 29.0 (BHA), 28.9 (BHA), 28.8 (BHA), 28.6 (BHA), 28.0 (Val-β), 24.9 (BHA), 22.0 (BHA), 20.1 (Thr-γ), 19.8 (Val-γa), 19.2 (Val-γb), 13.9 (BHA-16), 9.3 ppm (BHA-2′); IR (neat): $\tilde{\nu}$=3394, 3299, 3062, 2959, 2921, 2852, 1741, 1651, 1537, 1463 cm^{-1}; HRMS (ESI): m/z: calcd for $C_{36}H_{60}N_3O_7$: $[M+H]^+$: 646.4426; found: 646.4425.

1,3,4-Anhydro[L-valyl-L-threonyl-3-*O*-benzyl-L-seryl-(2*S*,3*R*)-2-methyl-3-hydroxyhexadecanoic acid] ((2*S*,3*R*)-13): Yield: 59.3 mg (91.8 μmol), 51%; $[\alpha]_D^{20}$=−37.8 (c=1 in $CHCl_3$); m.p.: 226°C; ^{1}H NMR (600 MHz, [D$_6$]DMSO): δ=8.05 (d, J=10.1 Hz, 1H; Val-NH), 7.88 (d, J=8.7 Hz, 1H; Ser-NH), 7.37 (d, J=9.7 Hz, 1H; Thr-NH), 7.35–7.23 (m, 5H; aromat. H), 5.14 (d, J=5.1 Hz, 1H; Thr-OH), 4.83 (ddd, J=10.0, 3.8, 3.0 Hz, 1H; BHA3-H), 4.63 (td, J=8.5, 4.2 Hz, 1H; Ser-H$^{\alpha}$), 4.53 (d, J= 12.6 Hz, 1H; Ser-CH_2Ph), 4.50 (d, J=12.6 Hz, 1H; Ser-CH_2Ph), 4.08 (dd, J=9.7, 3.4 Hz, 1H; Thr-H$^{\alpha}$), 4.01–3.96 (m, 1H; Thr-H$^{\beta}$), 3.97–3.91 (m, 1H; Val-H$^{\alpha}$), 3.71 (dd, J=9.8, 4.0 Hz, 1H; Ser-H$^{\beta}$a), 3.57 (dd, J=9.8, 4.4 Hz, 1H; Ser-H$^{\beta}$b), 2.47–2.44 (m, 1H; BHA2-H), 1.63–1.54 (m, 1H; BHA4a-H_2), 1.92–1.82 (m, 1H; Val-H$^{\beta}$), 1.45–1.36 (m, 1H; BHA4b-H_2), 1.26–1.14 (m, 22H; BHA5–15-H_2), 1.06 (d, J=6.3 Hz, 3H; Thr-H$^{\gamma}$), 1.02 (d, J=7.1 Hz, 3H; BHA2′-H_3), 0.90 (d, J=6.6 Hz, 1H; Val-H$^{\gamma}$a), 0.87 (d, J=6.5 Hz, 3H; Val-H$^{\gamma}$b), 0.82 ppm (t, J=7.0 Hz, 3H; BHA16-H_3); ^{13}C NMR (151 MHz, [D$_6$]DMSO): δ=170.9 (BHA-1, Val-1), 170.3 (Thr-1), 168.7 (Ser-1), 138.0 (aromat. C), 128.2 (aromat. C), 127.4 (aromat. C),

76.6 (BHA-3), 72.2 (Ser-CH_2Ph), 68.7 (Ser-β), 65.3 (Thr-β), 61.3 (Val-α), 59.7 (Thr-α), 51.4 (Ser-α), 43.2 (BHA-2), 31.2 (BHA), 29.4 (Val-β), 29.0 (BHA), 28.9 (BHA), 28.9 (BHA), 28.8 (BHA), 28.6 (BHA), 28.4 (BHA), 25.7 (BHA), 22.0 (BHA), 20.9 (Thr-γ), 19.1 (Val-γa), 19.0 (Val-γ*b*), 14.0 (BHA-2′), 13.9 ppm (BHA-16); IR: $\tilde{\nu}$ = 3311, 2963, 2919, 2852, 1726, 1673, 1642, 1556, 1508, 1469 cm^{-1}; HPLC-ESIMS (C4–70*;* t_R = 5.00 min): *m*/*z*: 646.41 [*M*+H]$^+$, 668.51 [*M*+Na]$^+$; HRMS (ESI): *m*/*z*: calcd for $C_{36}H_{60}N_3O_7$: 646.4426 [*M*+H]$^+$; found: 646.4424.

1,3.4-Anhydro[L-valyl-L-threonyl-3-*O*-benzyl-D-seryl-(2*S*,3*R*)-2-methyl-3-hydroxyhexadecanoic acid] ((2*S*,3*R*)-30): Yield: 9.3 mg (14.4 μmol), 8%; m.p.: 212°C; ^{1}H NMR (600 MHz, [D$_6$]DMSO): δ = 8.23 (d, *J* = 9.8 Hz, 1H; Val-NH), 7.62 (d, *J* = 9.3 Hz, 1H; Thr-NH), 7.35–7.17 (m, 5H; aromat. H), 7.09 (d, *J* = 6.5 Hz, 1H; Ser-NH), 4.96 (ddd, *J* = 10.4, 4.8, 2.6 Hz, 1H; BHA3-H), 4.87 (d, *J* = 4.5 Hz, 1H; Thr-OH), 4.44 (s, 2H; Ser-CH_2Ph), 4.40 (td, *J* = 6.2, 4.6 Hz, 1H; Ser-H^α), 4.30–4.24 (m, 1H; Thr-H^β), 4.15 (dd, *J* = 9.2, 2.9 Hz, 1H; Thr-H^α), 4.00 (t, *J* = 10.0 Hz, 1H; Val-H^α), 3.71 (dd, *J* = 9.5, 4.4 Hz, 1H; Ser-H^{β}a), 3.58 (dd, *J* = 9.5, 6.1 Hz, 1H; Ser-H^{β}b), 2.60–2.53 (m, 1H; BHA2-H), 1.88–1.74 (m, 2H; Val-H^β, BHA4a-H_2), 1.62–1.51 (m, 1H; BHA4b-H_2), 1.29–1.07 (m, 22H; BHA5–15-H_2), 1.04 (d, *J* = 7.1 Hz, 3H; BHA2′-H_3), 0.99 (d, *J* = 6.4 Hz, 3H; Thr-H^γ), 0.89 (d, *J* = 6.7 Hz, 3H; Val-H^{γ}a), 0.86 (d, *J* = 6.5 Hz, 3H; Val-H^{γ}b), 0.82 ppm (t, *J* = 7.0 Hz, 3H; BHA16-H_3); ^{13}C NMR (151 MHz, [D$_6$]DMSO): δ = 171.8 (Val-1), 171.5 (BHA-1), 169.5 (Thr-1), 167.4 (Ser-1), 137.6 (aromat. H), 128.0 (aromat. H), 127.4 (aromat. H), 127.2 (aromat. H), 76.5 (BHA-3), 72.2 (Ser-CH_2Ph), 68.9 (Ser-β), 63.9 (Thr-β), 60.8 (Val-α), 56.9 (Thr-α), 54.3 (Ser-α), 42.8 (BHA-2), 31.2 (BHA), 29.7 (Val-β), 29.0 (BHA), 28.9 (BHA), 28.8 (BHA), 28.6 (BHA), 28.1 (BHA), 25.4 (BHA), 22.0 (BHA), 20.5 (Thr-γ), 19.1 (Val-γa), 19.0 (Val-γb), 13.9 ppm (BHA-16, BHA-2′); IR (neat): $\tilde{\nu}$ = 3313, 2964, 2918, 2852, 1720, 1672, 1638, 1541, 1507, 1468 cm^{-1}; HPLC-ESIMS (C4–70; t_R = 5.57 min): *m*/*z*: 646.41, 668.53; HRMS (ESI): *m*/*z*: calcd for $C_{36}H_{60}N_3O_7$: 646.4426 [*M*+H]$^+$; found: 646.4425.

1,3.4-Anhydro[L-valyl-L-threonyl-3-*O*-benzyl-L-seryl-(2*S*,3*S*)-2-methyl-3-hydroxyhexadecanoic acid] ((2*S*,3*S*)-13): Yield: 72.1 mg (0.112 mmol), 62%; $[\alpha]_D^{20}$ = −58.2 (*c* = 1 in $CHCl_3$); m.p.: 235°C; ^{1}H NMR (600 MHz, [D$_6$]DMSO): δ = 8.01 (d, *J* = 8.2 Hz, 1H; Val-NH), 7.80 (d, *J* = 9.3 Hz, 1H; Thr-NH), 7.33–7.20 (m, 5H; aromat. H), 7.09 (d, *J* = 8.3 Hz, 1H; Ser-NH), 5.16 (d, *J* = 5.2 Hz, 1H; Thr-OH), 4.75 (ddd, *J* = 10.5, 5.0, 3.9 Hz, 1H; BHA3-H), 4.48 (d, *J* = 12.3 Hz, 1H; Ser-CH_2Ph), 4.46 (d, *J* = 12.3 Hz, 1H; Ser-CH_2Ph), 4.39 (ddd, *J* = 8.2, 6.9, 4.7 Hz, 1H; Ser-H^α), 4.09–4.02 (m, 2H; Thr-H^β, Thr-H^α), 3.73 (t, *J* = 8.6 Hz, 1H; Val-H^α), 3.62 (dd, *J* = 9.5, 4.7 Hz, 1H; Ser-H^{β}a), 3.46 (dd, *J* = 9.5, 6.9 Hz, 1H; Ser-H^{β}b), 2.72–2.61 (m, 1H; BHA2-H), 1.77–1.69 (m, 1H; BHA4a-H_2), 1.94–1.84 (m, 1H; Val-H^β), 1.50–1.41 (m, 1H; BHA4b-H_2), 1.28–1.08 (m, 22H; BHA5–15-H_3), 1.02 (d, *J* = 6.2 Hz, 3H; Thr-H^γ), 0.99 (d, *J* = 6.9 Hz, 3H; BHA2′-H_3), 0.93 (d, *J* = 6.6 Hz, 3H; Val-H^{γ}a), 0.88 (d, *J* = 6.8 Hz, 3H; Val-H^{γ}b), 0.82 ppm (t, *J* = 7.1 Hz, 3H; BHA16-H_3); ^{13}C NMR (151 MHz, [D$_6$]DMSO): δ = 173.3 (BHA-1), 171.6 (Val-1), 170.2 (Thr-1), 167.2 (Ser-1), 137.6 (*ipso*-aromat. C), 128.1 (2x *m*-aromat. C), 127.4 (*p*-aromat. C), 127.1 (2x *o*-aromat. C), 76.6 (BHA-3), 72.1 (Ser-CH_2Ph), 69.6 (Ser-β), 64.9 (Thr-β), 61.6 (Val-α), 59.5 (Thr-α), 53.3 (Ser-α), 42.8 (BHA-2), 31.2 (BHA), 29.9 (BHA), 29.1 (Val-β), 28.9 (7x BHA), 28.6 (BHA), 22.8 (BHA), 22.0 (BHA), 20.8 (Thr-γ), 19.3 (Val-γa), 19.0 (Val-γb), 14.7 (BHA-2′), 13.9 ppm (BHA-16); IR (neat): $\tilde{\nu}$ = 3333, 2958, 2921, 2852, 1739, 1660, 1530, 1503, 1469 cm^{-1}; HRMS (ESI): *m*/*z*: calcd for $C_{36}H_{60}N_3O_7$: 646.4426 [*M*+H]$^+$; found: 646.4425.

1,3.4-Anhydro[L-valyl-L-threonyl-3-*O*-benzyl-L-seryl-(2*R*,3*R*)-2-methyl-3-hydroxyhexadecanoic acid] ((2*R*,3*R*)-13): Yield: 41.8 mg (64.8 μmol), 36%; $[\alpha]_D^{20}$ = −49.3 (*c* = 0.5 in $CHCl_3$); m.p.: 234°C; ^{1}H NMR (600 MHz, [D$_6$]DMSO): δ = 7.94 (d, *J* = 10.1 Hz, 1H; Thr-NH), 7.72 (d, *J* = 9.0 Hz, 1H; Ser-NH), 7.60 (b, 1H; Val-NH), 7.40–7.20 (m, 5H; aromat. H), 5.21 (d, *J* = 4.6 Hz, 1H; Thr-OH), 4.77–4.73 (m, 1H; Ser-H^α), 4.70 (ddd, *J* = 8.0, 6.2, 2.0 Hz, 1H; BHA3-H), 4.54 (d, *J* = 12.4 Hz, 1H; Ser-CH_2Ph), 4.47 (d, *J* = 12.4 Hz, 1H; Ser-CH_2Ph), 4.11 (dd, *J* = 10.1, 2.6 Hz, 1H; Thr-H^α), 4.06 (m, 1H; Thr-H^β), 4.06–4.01 (m, 1H; Val-H^α), 3.84 (dd, *J* = 9.0, 2.6 Hz, 1H; Ser-H^{β}a), 3.59 (dd, *J* = 9.6, 3.0 Hz, 1H; Ser-H^{β}b), 2.58 (dq, *J* = 7.3, 1.90 Hz, 1H; BHA2-H), 2.09–1.95 (m, 1H; Val-H^β), 1.61–1.52 (m, 1H; BHA4a-H_2), 1.48–1.40 (m, 1H; BHA4b-H_2), 1.33–1.17 (m, 22H; BHA5–15-H_2), 1.13 (d, *J* = 7.3 Hz, 3H; BHA2′-H_3), 1.05 (d, *J* = 6.3 Hz, 3H; Thr-H^γ), 0.90 (d, *J* = 6.6 Hz, 3H; Val-H^{γ}a), 0.85 (d, *J* = 6.5 Hz, 3H; Val-H^{γ}b), 0.83 ppm (t, *J* = 7.0 Hz, 3H; BHA16-H_3); ^{13}C NMR (151 MHz, [D$_6$]DMSO): δ = 171.0 (BHA-1), 170.8 (Val-1), 170.3 (Thr-1), 168.9 (Ser-1), 137.9 (aromat. C), 129.8 (aromat. C), 128.1 (aromat. C), 127.3 (aromat. C), 77.9 (BHA-3), 72.4 (Ser-CH_2Ph), 70.0 (Ser-β), 65.2 (Thr-β), 61.3 (Val-α), 59.1 (Thr-α), 52.5 (Ser-α), 52.4, 42.8 (BHA-2), 40.0 (BHA), 31.7 (BHA), 31.2 (BHA), 29.0 (BHA), 29.1 (Val-β), 28.9 (BHA), 28.8 (BHA), 28.7 (BHA), 28.6 (BHA), 24.8 (BHA), 22.0 (BHA), 20.9 (Thr-γ), 19.2 (Val-γa), 18.9 (Val-γb), 13.9 ppm (BHA-16, BHA-2′); IR (neat): $\tilde{\nu}$ = 3285, 2923, 2853, 1725, 1684, 1637, 1544, 1455 cm^{-1}; HRMS (ESI): *m*/*z*: calcd for $C_{36}H_{60}N_3O_7$: 646.4426 [*M*+H]$^+$; found: 646.4425.

General procedure: Phosphorylation: Macrocyle **13** (20.5 mg, 31.7 μmol) and tetrazole (0.45 M in CH_3CN, 353 μL, 159 μmol) were dissolved in dry CH_2Cl_2 (634 μL) and stirred for 10 min at RT. Dibenzylisopropyl phosphoramidite[32] (626 μL, 190 μmol) was added and after 3 h, the mixture was cooled to 0°C, and a *t*BuOOH solution (5.5 M in hexane, 35 μL, 190 μmol) was added. The mixture was stirred for 15 min and quenched with 10% $Na_2S_2O_3$ (3 mL) at 0°C. The aqueous layer was extracted with ethyl acetate (4×3 mL) and the combined organic layers were dried with $MgSO_4$. After removal of the solvent, the crude product was purified by preparative HPLC and lyophilized to give a colorless powder. The obtained products were always found contaminated with minor amounts of monodebenzylated compound (1–5%), which were apparent in the ^{31}P NMR at ca. δ = −6 ppm.

1,3.4-Anhydro[L-valyl-3-*O*-dibenzylphospho-L-threonyl-3-*O*-benzyl-L-seryl-(2*S*,3*R*)-2-methyl-3-hydroxyhexadecanoic acid] ((2*S*,3*R*)-28): Yield: 20.1 mg (22.2 μmol), 70%; ^{1}H NMR (400 MHz, $CDCl_3$): δ = 7.63 (d, *J* = 6.2 Hz, 1H; Ser-NH), 7.35–7.15 (m, 15H; aromat. H), 7.00 (d, *J* = 7.1 Hz, 1H; Thr-NH), 6.46 (brs, 1H; Val-NH), 5.41–5.30 (m, 1H; Thr-H^β), 4.98–4.89 (m, 5H; $POCH_2$Ph, BHA3-H), 4.50 (td, *J* = 7.1, 2.0 Hz, 1H; Ser-H^α), 4.32 (d, *J* = 10.8 Hz, 1H; Ser-CH_2Ph), 4.24 (d, *J* = 10.8 Hz, 1H; Ser-CH_2Ph), 4.23–4.18 (m, 1H; Thr-H^α), 4.15 (t, *J* = 10.5 Hz, 1H; Val-H^α), 3.88 (dd, *J* = 9.2, 2.1 Hz, 1H; Ser-H^{β}a), 3.70 (dd, *J* = 9.2, 2.3 Hz, 1H; Ser-H^{β}b), 2.24–2.15 (m, 1H; BHA2-H), 1.73–1.60 (m, 2H; Val-H^β, BHA4a-H_2), 1.59–1.49 (m, 1H; BHA4b-H_2), 1.32 (d, *J* = 6.5 Hz, 3H; Thr-H^γ), 1.25–1.13 (m, 25H; BHA), 1.05 (d, *J* = 7.1 Hz, 3H; BHA2′-H_3), 0.88 (d, *J* = 6.6 Hz, 3H; Val-H^{γ}a), 0.81 (t, *J* = 7.0 Hz, 3H; BHA16-H_3), 0.79 ppm (d, *J* = 6.5 Hz, 3H; Val-H^{γ}b); ^{31}P NMR (162.1 MHz, $CDCl_3$): δ = −1.26 ppm.

1,3.4-Anhydro[L-valyl-3-*O*-dibenzylphospho-L-threonyl-3-*O*-benzyl-L-seryl-(2*R*,3*R*)-2-methyl-3-hydroxyhexadecanoic acid] ((2*R*,3*R*)-28): Yield: 22.1 mg (24.4 μmol), 80%; ^{1}H NMR (400 MHz, $CDCl_3$): δ = 7.67 (d, *J* = 6.8 Hz, 1H; Ser-NH), 7.24 (m, 15H; aromat. H), 7.08 (d, *J* = 7.0 Hz, 1H; Thr-NH), 6.04 (d, *J* = 9.1 Hz, 1H; Val-NH), 5.44–5.32 (m, 1H; Thr-H^β), 4.99–4.92 (m, 4H; $POCH_2$Ph), 4.71 (t, *J* = 6.7 Hz, 1H; BHA3-H), 4.47 (td, *J* = 7.3, 2.2 Hz, 1H; Ser-H^α), 4.36 (d, *J* = 10.7 Hz, 1H; Ser-CH_2Ph), 4.25 (d, *J* = 10.7 Hz, 1H; Ser-CH_2Ph), 4.18–4.01 (m, 2H; Thr-H^α, Val-H^α), 3.86 (dd, *J* = 9.1, 2.2 Hz, 1H; Ser-H^{β}a), 3.65 (dd, *J* = 9.1, 2.5 Hz, 1H; Ser-H^{β}b), 2.56 (dq, *J* = 7.1, 0.55 Hz, 1H; BHA2-H), 1.95–1.82 (m, 1H; Val-H^β), 1.76–1.55 (m, 2H; BHA4-H_2), 1.31 (d, *J* = 6.5 Hz, 3H; Thr-H^γ), 1.26–1.09 (m, 25H; BHA, BHA2′-H_3), 0.91 (d, *J* = 6.6 Hz, 3H; Val-H^{γ}a), 0.82 (d, *J* = 6.0 Hz, 3H; Val-H^{γ}a), 0.81 ppm (t, *J* = 6.5 Hz, 3H; BHA16-H_3); ^{31}P NMR (162.1 MHz, $CDCl_3$): δ = −1.10 ppm.

1,3.4-Anhydro[L-valyl-3-*O*-dibenzylphospho-L-threonyl-3-*O*-benzyl-L-seryl-(2*S*,3*S*)-2-methyl-3-hydroxyhexadecanoic acid] ((2*S*,3*S*)-28): Yield: 23.8 mg (26.3 μmol), 84%; ^{1}H NMR (400 MHz, $CDCl_3$): δ = 7.70 (brs, 1H; Thr-NH), 7.37–7.02 (m, 15H; aromat. H), 6.87 (bs, 1H; Ser-NH), 6.30 (brs, 1H; Val-NH), 5.02 (ddd, *J* = 14.4, 6.6, 3.9 Hz, 1H; Thr-H^β), 4.96–4.87 (m, 5H; BHA3-H, $POCH_2$Ph), 4.51 (dd, *J* = 9.0, 3.4 Hz, 1H; Thr-H^α), 4.44 (dd, *J* = 9.8, 5.4 Hz, 1H; Ser-H^α), 4.26 (d, *J* = 1.7 Hz, 2H; Ser-CH_2Ph), 4.02–3.94 (m, 1H; Val-H^α), 3.70 (dd, *J* = 9.5, 4.0 Hz, 1H; Ser-H^{β}a), 3.60 (dd, *J* = 9.5, 5.6 Hz, 1H; Ser-H^{β}b), 2.59 (qd, *J* = 13.9, 6.9 Hz, 1H; BHA2-H), 2.04–1.77 (m, 2H; Val-H^β, BHA4a-H_2), 1.44 (ddd, *J* = 14.9, 10.3, 5.1 Hz, 1H; BHA4b-H_2), 1.31 (d, *J* = 6.6 Hz, 3H; Thr-H^γ), 1.28–1.12 (m, 22H; BHA), 1.11 (d, *J* = 6.9 Hz, 3H; BHA2′-H_3), 0.97 (d, *J* = 6.6 Hz, 3H; Val-H^{γ}a), 0.93 (d, *J* = 6.7 Hz, 3H; Val-H^{γ}b), 0.81 ppm (t,

J=6.9 Hz, 3H; BHA16-H_3); ^{31}P NMR (162.1 MHz, $CDCl_3$): δ = −1.11 ppm.

1,3,4-Anhydro[L-valyl-3-*O*-dibenzylphospho-L-threonyl-3-*O*-benzyl-L-seryl-(2*R*,3*S*)-2-methyl-3-hydroxyhexadecanoic acid] ((2*R*,3*S*)-28): Yield: 21.8 mg (24.1 μmol), 76%; ^{1}H NMR (400 MHz, $CDCl_3$): δ = 8.14 (brs, 1H; Thr-NH), 7.42–6.99 (m, 15H; aromat. H), 6.80 (brs, 1H; Ser-NH), 6.43 (brs, 1H; Val-NH), 5.24–5.15 (m, 1H; BHA3-H), 5.02 (ddd, J = 16.7, 6.4, 3.4 Hz, 1H; Thr-H$^\beta$), 4.93–4.81 (m, 4H; $POCH_2Ph$), 4.53–4.44 (m, 2H; Thr-H$^\alpha$, Ser-H$^\alpha$), 4.29 (d, J = 12.0 Hz, 1H; Ser-CH_2Ph), 4.22 (d, J = 12.0 Hz, 1H; Ser-CH_2Ph), 4.00 (t, J = 8.4 Hz, 1H; Val-H$^\alpha$), 3.65 (dd, J = 9.5, 4.4 Hz, 1H; Ser-H$^\beta$a), 3.55 (dd, J = 8.8, 6.9 Hz, 1H; Ser-H$^\beta$b), 2.76–2.59 (m, 1H; BHA2-H), 2.09–1.97 (m, 1H; Val-H$^\beta$), 1.98–1.69 (m, 2H; BHA4-H_2), 1.32 (d, J = 6.8 Hz, 3H; Thr-H$^\gamma$), 1.21 (d, J = 7.4 Hz, 3H; BHA2′-H_3), 1.18 (s, 22H; BHA), 1.00–0.90 (m, 6H; Val-H$^\gamma$), 0.81 ppm (t, J = 6.7 Hz, 3H; BHA16-H_3); ^{31}P NMR (162.1 MHz, $CDCl_3$): δ = −1.24 ppm.

General procedure: Debenzylation of phosphorylated depsipeptides: Phosphotriester **28** (19.0 mg, 20.97 μmol) was dissolved in EtOH (3 mL). 10% Pd/C (7 mg) was added and the mixture was hydrogenated (H_2 balloon) for 4 h. Filtration through a pad of Celite and evaporation of the solvent gave product **14** as a colorless oil.

1,3,4-Anhydro[L-valyl-phospho-L-threonyl-L-seryl-(2*S*,3*R*)-2-methyl-3-hydroxyhexadecanoic acid] ((2*S*,3*R*)-14): Yield: 8.2 mg (14.7 μmol), 87%; ^{1}H NMR (600 MHz, [D$_6$]DMSO): δ = 8.15 (d, J = 8.6 Hz, 1H; Val-NH), 8.01 (d, J = 7.9 Hz, 1H; Ser-NH), 7.61 (d, J = 8.9 Hz, 1H; Thr-NH), 4.85–4.77 (m, 1H; BHA3-H), 4.53–4.47 (m, 1H; Thr-H$^\beta$), 4.45 (dt, J = 8.7, 4.3 Hz, 1H; Ser-H$^\alpha$) 4.19 (dd, J = 9.0, 4.6 Hz, 1H; Thr-H$^\alpha$), 3.97 (dd, J = 10.7, 10.7 Hz, 1H; Val-H$^\alpha$), 3.72 (dd, J = 11.3, 4.5 Hz, 1H; Ser-H$^\beta$a), 3.62 (dd, J = 11.3, 4.1 Hz, 1H; Ser-H$^\beta$b), 2.47–2.43 (m, 1H; BHA2-H), 1.96–1.80 (m, 1H; Val-H$^\beta$), 1.63–1.51 (m, 1H; BHA4a-H_2), 1.42–1.29 (m, 1H; BHA4b-H_2), 1.30–1.12 (m, 25H; Thr-H$^\gamma$, BHA), 1.03 (d, J = 7.0 Hz, 1H; BHA2′-H_3), 0.91 (d, J = 6.6 Hz, 3H; Val-H$^\gamma$a), 0.88 (d, J = 6.6 Hz, 3H; Val-H$^\gamma$b), 0.85 ppm (t, J = 6.9 Hz, 3H; BHA16-H_3); ^{13}C NMR (151 MHz, [D$_6$]DMSO): δ = 170.8 (BHA-1, Val-1), 169.0 (Ser-1), 168.8 (Thr-1), 76.3 (BHA-3), 71.1 (Thr-β), 61.3 (Val-α), 60.3 (Ser-β), 59.3 (Thr-α), 53.4 (Ser-α), 43.3 (BHA-2), 31.3 (BHA), 29.3 (Val-β), 29.0 (BHA), 28.9 (BHA), 28.8 (BHA), 28.7 (BHA), 28.5 (BHA), 25.7 (BHA), 22.1 (BHA), 19.1 (Val-γ), 18.9 (Thr-γ), 13.9 ppm (BHA-2′, BHA-16); ^{31}P NMR (162.1 MHz, $CDCl_3$): δ = −0.46; HPLC-ESIMS (C4–50, t_R = 6.35 min): m/z: 636.12 [M+H]$^+$, 658.33 [M+Na]$^+$; HRMS (ESI): m/z: calcd for $C_{29}H_{55}N_3O_{10}P$: 636.3620 [M+H]$^+$; found: 636.3619.

1,3,4-Anhydro[L-valyl-phospho-L-threonyl-L-seryl-(2*R*,3*S*)-2-methyl-3-hydroxyhexadecanoic acid] ((2*R*,3*S*)-14): Yield: 13.1 mg (20.3 μmol), 97%; ^{1}H NMR (600 MHz, [D$_6$]DMSO): δ = 9.01 (d, J = 6.3 Hz, 1H; Thr-NH), 8.38 (brs, 1H; Val-NH), 7.69 (brs, 1H; Ser-NH), 4.75 (ddd, J = 7.5, 4.8, 1.7 Hz, 1H; BHA3-H), 4.58–4.47 (m, 1H; Thr-H$^\beta$), 4.32 (td, J = 9.8, 6.1 Hz, 1H; Ser-H$^\alpha$), 4.05 (dd, J = 9.0, 2.2 Hz, 1H; Thr-H$^\alpha$), 3.87 (dd, J = 10.8, 9.8 Hz, 1H; Val-H$^\alpha$), 3.59–3.45 (m, 2H; Ser-H$^\beta$), 2.50 (m, 1H; BHA2-H), 2.24–2.13 (m, 1H; Val-H$^\beta$), 1.77–1.63 (m, 1H; BHA4a-H_2), 1.47–1.35 (m, 1H; BHA4b-H_2), 1.32–1.12 (m, 28H; BHA2′-H_3, BHA, Thr-H$^\gamma$), 0.93–0.73 ppm (m, 9H; Val-H$^\gamma$, BHA16-H_3); ^{13}C NMR (151 MHz, [D$_6$]DMSO): δ = 172.2 (BHA-1), 171.6 (Val-1), 170.1 (Thr-1), 168.8 (Ser-1), 76.1 (BHA-3), 69.2 (Thr-β), 62.0 (Ser-β, Val-α), 59.6 (Thr-α), 55.8 (Ser-α), 43.0 (BHA-2), 31.3 (BHA), 29.8 (BHA), 29.0 (BHA), 28.9 (BHA), 28.8 (BHA), 28.7 (Val-β), 24.4 (BHA), 22.1 (BHA), 19.6 (Thr-γ), 19.1 (Val-γ), 13.9 (BHA-16), 8.8 ppm (BHA-2′); ^{31}P NMR (162.1 MHz, $CDCl_3$): δ = −0.87 ppm; HPLC-ESIMS (C4–50, t_R = 5.98 min): m/z: 636.15 [M+H]$^+$, 658.35 [M+Na]$^+$; HRMS (ESI): m/z: calcd for $C_{29}H_{55}N_3O_{10}P$: 636.3620 [M+H]$^+$; found: 636.3619.

1,3,4-Anhydro[L-valyl-phospho-L-threonyl-L-seryl-(2*S*,3*S*)-2-methyl-3-hydroxyhexadecanoic acid] ((2*S*,3*S*)-14): Yield: 13.3 mg (24.0 μmol), 95%; ^{1}H NMR (600 MHz, [D$_6$]DMSO): δ = 8.59 (d, J = 6.0 Hz, 1H; Val-NH), 8.37 (d, J = 8.6 Hz, 1H; Thr-NH), 7.33 (d, J = 8.7 Hz, 1H; Ser-NH), 4.66 (td, J = 9.3, 4.4 Hz, 1H; BHA3-H), 4.58–4.51 (m, 1H; Thr-H$^\beta$), 4.25 (td, J = 9.4, 5.5 Hz, 1H; Ser-H$^\alpha$), 4.11 (dd, J = 8.8, 4.1 Hz, 1H; Thr-H$^\alpha$), 3.72 (dd, J = 9.3, 9.3 Hz, 1H; Val-H$^\alpha$), 3.52 (d, J = 5.5 Hz, 2H; Ser-H$^\beta$), 2.76 (qd, J = 13.7, 6.7 Hz, 1H; BHA2-H), 2.07–1.95 (m, 1H; Val-H$^\beta$), 1.78–1.67 (m, 1H; BHA4a-H_2), 1.50–1.39 (m, 1H; BHA4b-H_2), 1.32–1.14 (m, 25H; BHA, Thr-H$^\gamma$), 0.97 (d, J = 6.9 Hz, 1H; BHA2′-H_3), 0.92 (d, J = 6.5 Hz, 3H; Val-H$^\gamma$a), 0.88 (d, J = 6.5 Hz, 3H; Val-H$^\gamma$b), 0.85 ppm (t, J = 6.7 Hz, 3H; BHA16-H_3); ^{13}C NMR (151 MHz, [D$_6$]DMSO): δ = 173.3 (BHA-1), 171.8 (Val-1), 169.4 (Thr-1), 168.1 (Ser-1), 76.5 (BHA-3), 69.5 (Thr-β), 62.0 (Ser-β), 61.8 (Val-α), 59.6 (Thr-α), 55.7 (Ser-α), 42.9 (BHA-2), 31.2 (BHA), 30.0 (BHA-4), 29.1 (BHA), 29.0 (Val-β), 28.8 (BHA), 28.7 (BHA), 22.6 (BHA), 22.0 (BHA), 19.5 (Val-γa), 19.4 (Thr-γ), 19.1 (Val-γb), 14.5 (BHA-2′), 13.9 ppm (BHA-16); ^{31}P NMR (162.1 MHz, $CDCl_3$): δ = −0.37; HPLC-ESIMS (C4–50, t_R = 5.52 min): m/z: 636.12 [M+H]$^+$, 658.35 [M+Na]$^+$; HRMS (ESI): m/z: calcd for $C_{29}H_{55}N_3O_{10}P$: 636.3620 [M+H]$^+$; found: 636.3619.

1,3,4-Anhydro[L-valyl-phospho-L-threonyl-L-seryl-(2*R*,3*R*)-2-methyl-3-hydroxyhexadecanoic acid) ((2*R*,3*R*)-14): Yield: 12.8 mg (23.1 μmol), 95%; ^{1}H NMR (600 MHz, [D$_6$]DMSO): δ = 8.79–8.41 (m, 2H; Ser-NH, Thr-NH) 8.26 (brs, 1H; Val-NH), 4.64 (t, J = 6.6 Hz, 1H; BHA3-H), 4.59–4.46 (m, 2H; Ser-H$^\alpha$, Thr-H$^\beta$), 4.15 (d, J = 9.5 Hz, 1H; Thr-H$^\alpha$), 4.01 (dd, J = 10.8, 10.8 Hz, 1H; Val-H$^\alpha$), 3.75 (dd, J = 11.2, 6.0 Hz, 1H; Ser-H$^\beta$a), 3.61 (dd, J = 10.9, 2.3 Hz, 1H; Ser-H$^\beta$b), 2.53–2.51 (m, 1H; BHA2-H), 2.22–2.13 (m, 1H; Val-H$^\beta$), 1.56–1.44 (m, 1H; BHA4a-H_2), 1.42–1.32 (m, 1H; BHA4b-H_2), 1.32–1.08 (m, 28H; BHA2′-H_3, BHA, Thr-H$^\gamma$), 0.89 (d, J = 6.5 Hz, 3H; Val-H$^\gamma$a), 0.85 (t, J = 6.8 Hz, 3H; BHA16-H_3), 0.84 ppm (d, J = 6.2 Hz, 3H; Val-H$^\gamma$b); ^{13}C NMR (151 MHz, [D$_6$]DMSO): δ = 171.2 (Val-1), 170.2 (BHA-1), 170.0 (Thr-1), 169.7 (Ser-1), 76.9 (BHA-3), 70.0 (Thr-β), 61.6 (Val-α), 61.5 (Ser-β), 59.1 (Thr-α), 54.5 (Ser-α), 43.5 (BHA-2), 32.0 (BHA-4), 31.2 (BHA), 29.0 (BHA), 28.9 (BHA), 28.7 (BHA), 28.5 (Val-β), 25.0 (BHA), 22.0 (BHA), 20.0 (Thr-γ), 19.2 (Val-γa), 19.0 (Val-γb), 14.1 (BHA-2′), 13.9 ppm (BHA-16); ^{31}P NMR (162.1 MHz, [D$_6$]DMSO): δ = −1.26 ppm; HPLC-ESIMS (C4–50; t_R = 6.98 min): m/z: 636.16 [M+H]$^+$, 658.35 [M+Na]$^+$; HRMS (ESI): m/z: calcd for $C_{29}H_{55}N_3O_{10}P$: 636.3620 [M+H]$^+$; found: 636.3618.

1,3,4-Anhydro[L-valyl-L-threonyl-L-seryl-(2*S*,3*R*)-2-methyl-3-hydroxyhexadecanoic acid] ((2*S*,3*R*)-29): Benzylated cylodepsipeptide **13** (15.8 mg, 24.6 μmol) was dissolved in EtOH (2.5 mL). 10% Pd/C (7 mg) and HCl (25 μL, 1 N) were added and the mixture was hydrogenated (H_2 balloon) for 4 h. Filtration through a pad of Celite and evaporation of the solvent gave product **29** as a colorless solid. Yield: 12.4 mg (22.4 μmol), 91%; R_f: 0.27 (CH_2Cl_2/MeOH 10:1, v/v); $[\alpha]_D^{20}$ = −30.0 (c = 0.5 in 1:1 MeOH/$CHCl_3$); ^{1}H NMR (600 MHz, [D$_6$]DMSO): δ = 8.12 (d, J = 10.1 Hz, 1H; Val-NH), 7.83 (d, J = 8.7 Hz, 1H; Ser-NH), 7.46 (d, J = 9.8 Hz, 1H; Thr-NH), 5.10 (d, J = 5.1 Hz, 1H; Thr-OH), 4.88–4.77 (m, 2H; Ser-OH, BHA3-H), 4.49–4.42 (m, 1H; Ser-H$^\alpha$), 4.10 (dd, J = 9.8, 3.0 Hz, 1H; Thr-H$^\alpha$), 4.06–3.94 (m, 2H; Thr-H$^\beta$, Val-Ha), 3.78 (ddd, J = 10.2, 5.5, 3.6 Hz, 1H; Ser-H$^\beta$a), 3.57 (dd, J = 10.8, 4.5 Hz, 1H; Ser-H$^\beta$b), 2.48–2.43 (m, 1H; BHA2-H), 1.91 (dq, J = 13.0, 6.5 Hz, 1H; Val-H$^\beta$), 1.67–1.56 (m, 1H; BHA4a-H_2), 1.46–1.33 (m, 1H; BHA4b-H_2), 1.33–1.11 (m, 22H; BHA), 1.07 (d, J = 6.3 Hz, 3H; Thr-H$^\gamma$), 1.04 (d, J = 7.1 Hz, 3H; BHA2′-H_3), 0.92 (d, J = 8.8 Hz, 3H; Val-H$^\gamma$a), 0.90 (d, J = 8.6 Hz, 3H; Val-H$^\gamma$b), 0.85 ppm (t, J = 6.7 Hz, 3H; BHA16-H_3); ^{13}C NMR (151 MHz, [D$_6$]DMSO): δ = 170.9 (BHA-1), 170.8 (Val-1), 170.1 (Thr-1), 169.0 (Ser-1), 76.3 (BHA-3), 65.3 (Thr-β), 61.5 (Thr-α), 61.1 (Ser-β), 60.2 (Val-α), 53.5 (Ser-α), 43.1 (BHA-2), 39.7 (Val-β), 31.2 (BHA), 28.9 (BHA), 28.9 (BHA), 28.9 (BHA), 28.8 (BHA), 28.6 (BHA), 25.7 (BHA), 22.0 (BHA), 20.7 (Thr-γ), 19.1 (Val-γa), 19.0 (Val-γb), 13.9 ppm (BHA-16; BHA-2′); IR (neat): $\tilde{\nu}$ = 3444, 3333, 3085, 2922, 2852, 1729, 1656, 1550, 1466, 1367 cm^{-1}; HRMS (ESI): m/z: calcd for $C_{29}H_{54}N_3O_7$: 556.3956 [M+H]$^+$; found: 556.3950.

NMR spectroscopic experiments: All spectra were recorded at RT on a Varian Mercury-Vx 400 MHz or a Varian Unity Inova 600 MHz NMR spectrometer. For signal assignment ^{1}H-, APT, TOCSY, gHSQC, and gHMBC spectra were recorded. ROESY experiments have been performed with 6 mg depsipeptide in 0.5 mL degassed [D$_6$]DMSO at a mixing time of 300 ms. Integration of the signals was performed with the program Aurelia from Bruker and the integrated volumes were offset corrected.[60] Proton–proton distances were calculated and ranked by using two methylene protons as reference (1.8 Å).

Computational methods: The low-energy conformations of the cyclic depsipeptides were calculated by using the programs Macromodel 9.1[37] and Maestro. A total of 35,000 starting structures was generated for each molecule by using the LMOD method with low-frequency eigenvector

sampling.[36] All ring atoms as well as the first atoms of the side chains were used for the identification of new unique structures applying a root-mean-square deviation (RMSD) threshold of 0.25 Å. All conformers within an energy window of 50 kJ mol^{-1} were used. Subsequently, energy minimization with the truncated Newton conjugated gradient (TNCG)[61] was performed on each conformer by using the OPLS 2005 force field[62] with implemented GB/SA solvation model.[63] The line search parameter was set from 1 to 0 to choose the direction of minimization steps, default values were used for the remaining parameters. Convergence (RMSD gradient = 0.05 kJ mol^{-1} Å^{-1}) was reached after a maximum of 10,000 iterations. For the restrained modeling up to 30 distances calculated from NOE signals were set as distance constraints with a ±10% flat potential interval. Calculations starting from varying initial geometries gave consistent results and each unique conformation was found on average 20–30 times. The final conformations were submitted to a clustering by using Schrödinger's XCluster program. Clustering criterion was the atomic root-mean-square (RMS) with all heavy ring atoms and the first heavy atom of each substituent as comparison set. Subsequently, the hierarchy level corresponding to an RMS of 0.1 Å was chosen and its representative structures, the cluster centers, exported. Images were created by using PyMol 0.99 from Delano Scientific. Overlays were generated based on all heavy atoms in the macrocycle by using Schrödinger Maestro 7.5.

Inhibition studies: The human VHR (≈12.5 mg mL^{-1}) was prepared according to published procedures.[51] 10 mM stock solutions of inhibitors were prepared in DMSO. The assay buffer consisted of 25 mM MOPS, 5 mM EDTA, 1 mM DTE, and 0.025% NP-40. The pH was adjusted to 6.5 and the buffer was filtered and degassed. 10 mM *p*NPP was used as substrate. In a 96-well plate a dilution series of 50 µL inhibitor was pipetted. After addition of 30 µL VHR (final dilution 1:1600), the mixture was incubated at 37 °C for 30 min. As soon as 20 µL *p*NPP was added, the extinction was monitored for 40 min in 2 min steps at 405 nm. Subsequently, an endpoint measurement was performed. To this end, 10 µL 2 N NaOH were added to each well and the extinction was measured again. All experiments were carried out in triplicate, including the known PTP inhibitor IV[64] as control. To determine the IC_{50} values, experimental data were analyzed by using the ORIGIN (Microcal Software) program.

Malachite green test:[59] The malachite green solution was prepared by addition of malachite green oxalate (350 mg, 0.38 mmol) and ammonium molybdate (3.2 g, 2.59 mmol) to 33% HCl (45 mL). The mixture was diluted with water to 150 mL, stirred for 12 h, and filtrated twice. The same assay conditions as for the IC_{50} determination without addition of the substrate were applied. After 45 min, 50 µL malachite green solution was added and the mixture was incubated for an additional 15 min at RT. For calibration, a series of defined Na_2HPO_4 concentrations were measured. The phosphate concentration was monitored by UV-absorbance at 620 nm.

Acknowledgements

This research was supported by the Zentrum für Angewandte Chemische Genomic, the Max-Planck Gesellschaft (to H. Waldmann) and the DFG (Emmy-Noether Young Investigator grant to H.-D. Arndt). S. Wetzel was supported by a Novartis graduate fellowship. We thank Dr. K. Alexandrov (Max-Planck-Institute Dortmund) for enzyme preparation and purification.

[1] Y. Suarez, L. Gonzalez, A. Cuadrado, M. Berciano, M. Lafarga, A. Munoz, *Mol. Cancer Ther.* **2003**, *2*, 863–872.
[2] H. Kogen, T. Kiho, M. Nakayama, Y. Furukawa, T. Kinoshita, M. Inukai, *J. Am. Chem. Soc.* **2000**, *122*, 10214–10215.
[3] I. K. Dev, R. J. Harvey, P. H. Ray, *J. Biol. Chem.* **1985**, *260*, 5891–5894.
[4] *Dictionary of Natural Products*, 16.1 ed., Chapman & Hall/CRC press, London, **2008**.
[5] X. Huang, E. Roemer, I. Sattler, U. Moellmann, A. Christner, S. Grabley, *Angew. Chem.* **2006**, *118*, 3138–3143; *Angew. Chem. Int. Ed.* **2006**, *45*, 3067–3072.
[6] I. Namatame, H. Tomoda, S. Ishibashi, S. Omura, *Proc. Natl. Acad. Sci. USA* **2004**, *101*, 737–742.
[7] T. Morino, A. Masuda, M. Yamada, M. Nishimoto, T. Nishikiori, S. Saito, N. Shimada, *J. Antibiot.* **1994**, *47*, 1341–1343.
[8] T. Hamaguchi, A. Masuda, T. Morino, H. Osada, *Chem. Biol.* **1997**, *4*, 279–286.
[9] D. R. March, G. Abbenante, D. A. Bergman, R. I. Brinkworth, W. Wickramasinghe, J. Begun, J. L. Martin, D. P. Fairlie, *J. Am. Chem. Soc.* **1996**, *118*, 3375–3379.
[10] C. Gilon, D. Halle, M. Chorev, Z. Selinger, G. Byk, *Biopolymers* **1991**, *31*, 745–750.
[11] V. J. Hruby, F. Alobeidi, W. Kazmierski, *Biochem. J.* **1990**, *268*, 249–262.
[12] J. Chatterjee, D. Mierke, H. Kessler, *J. Am. Chem. Soc.* **2006**, *128*, 15164–15172.
[13] H. Kessler, R. Gratias, G. Hessler, M. Gurrath, G. Müller, *Pure Appl. Chem.* **1996**, *68*, 1201–1205.
[14] M. P. Glenn, M. J. Kelso, J. D. A. Tyndall, D. P. Fairlie, *J. Am. Chem. Soc.* **2003**, *125*, 640–641.
[15] D. F. Veber, S. R. Johnson, H. Y. Cheng, B. R. Smith, K. W. Ward, K. D. Kopple, *J. Med. Chem.* **2002**, *45*, 2615–2623.
[16] T. J. Styers, R. Rodriguez, P. S. Pan, S. R. McAlpine, *Tetrahedron Lett.* **2006**, *47*, 515–517.
[17] A. R. Dentino, P. A. Raj, K. K. Bhandary, M. E. Wilson, M. J. Levine, *J. Biol. Chem.* **1991**, *266*, 18460–18468.
[18] R. Sakai, K. L. Rinehart, V. Kishore, B. Kundu, G. Faircloth, J. B. Gloer, J. R. Carney, M. Namikoshi, F. Sun, R. G. Hughes, D. G. Gravalos, T. G. de Quesada, G. R. Wilson, R. M. Heid, *J. Med. Chem.* **1996**, *39*, 2819–2834.
[19] F. Cavelierfrontin, G. Pepe, J. Verducci, D. Siri, R. Jacquier, *J. Am. Chem. Soc.* **1992**, *114*, 8885–8890.
[20] R. E. Shute, M. Kawai, D. H. Rich, *Tetrahedron* **1988**, *44*, 685–695.
[21] E. Pinet, J. M. Neumann, I. Dahse, G. Girault, F. Andre, *Biopolymers* **1995**, *36*, 135–152.
[22] M. Kawai, R. S. Pottorf, D. H. Rich, *J. Med. Chem.* **1986**, *29*, 2409–2411.
[23] M. Manger, M. Scheck, H. Prinz, J. P. von Kries, T. Langer, K. Saxena, H. Schwalbe, A. Furstner, J. Rademann, H. Waldmann, *ChemBioChem* **2005**, *6*, 1749–1753.
[24] A. Abiko, J. F. Liu, S. Masamune, *J. Am. Chem. Soc.* **1997**, *119*, 2586–2587.
[25] D. A. Evans, J. Bartroli, T. L. Shih, *J. Am. Chem. Soc.* **1981**, *103*, 2127–2129.
[26] D. A. Evans, J. V. Nelson, E. Vogel, T. R. Taber, *J. Am. Chem. Soc.* **1981**, *103*, 3099–3111.
[27] T. Inoue, J. F. Liu, D. C. Buske, A. Abiko, *J. Org. Chem.* **2002**, *67*, 5250–5256.
[28] M. J. Mckennon, A. I. Meyers, K. Drauz, M. Schwarm, *J. Org. Chem.* **1993**, *58*, 3568–3571.
[29] J. R. Gage, D. A. Evans, *Org. Synth.* **1990**, *68*, 77–82.
[30] D. B. Dess, J. C. Martin, *J. Org. Chem.* **1983**, *48*, 4155–4156.
[31] J. Inanaga, K. Hirata, H. Saeki, T. Katsuki, M. Yamaguchi, *Bull. Chem. Soc. Jpn.* **1979**, *52*, 1989–1993.
[32] J. W. Perich, R. B. Johns, *Tetrahedron Lett.* **1988**, *29*, 2369–2372.
[33] D. S. Wishart, B. D. Sykes, F. M. Richards, *J. Mol. Biol.* **1991**, *222*, 311–333.
[34] A. Pardi, M. Billeter, K. Wüthrich, *J. Mol. Biol.* **1984**, *180*, 741–751.
[35] M. Karplus, *J. Am. Chem. Soc.* **1963**, *85*, 2870–2871.
[36] I. Kolossvary, W. C. Guida, *J. Am. Chem. Soc.* **1996**, *118*, 5011–5019.
[37] F. Mohamadi, N. G. J. Richards, W. C. Guida, R. Liskamp, M. Lipton, C. Caufield, G. Chang, T. Hendrickson, W. C. Still, *J. Comput. Chem.* **1990**, *11*, 440–467.
[38] D. Barford, L. N. Johnson, *Protein Sci.* **1992**, *1*, 472–493.
[39] P. Rajagopal, E. B. Waygood, R. E. Klevit, *Biochemistry* **1994**, *33*, 15271–15282.

[40] S. R. Sprang, K. R. Acharya, E. J. Goldsmith, D. I. Stuart, K. Varvill, R. J. Fletterick, N. B. Madsen, L. N. Johnson, *Nature* **1988**, *336*, 215–221.
[41] R. M. Wynn, M. Kato, M. Machius, J. L. Chuang, L. Jun, D. R. Tomchick, D. T. Chuang, *Structure* **2004**, *12*, 2185–2196.
[42] A. Tholey, A. Lindemann, V. Kinzel, J. Reed, *Biophys. J.* **1999**, *76*, 76–87.
[43] F. Schumann, A. Müller, M. Koksch, G. Muller, N. Sewald, *J. Am. Chem. Soc.* **2000**, *122*, 12009–12010.
[44] H. Weisshoff, C. Prasang, P. Henklein, C. Frommel, A. Zschunke, C. Mügge, *Eur. J. Biochem.* **1999**, *259*, 776–788.
[45] M. Pfaff, K. Tangemann, B. Müller, M. Gurrath, G. Müller, H. Kessler, R. Timpl, J. Engel, *J. Biol. Chem.* **1994**, *269*, 20233–20238.
[46] M. Malesevic, Z. Majer, E. Vass, T. Huber, U. Strijowski, M. Hollosi, N. Sewald, *Int. J. Pept. Res. Ther.* **2006**, *12*, 165–177.
[47] M. Heller, M. Sukopp, N. Tsomaia, M. John, D. F. Mierke, B. Reif, H. Kessler, *J. Am. Chem. Soc.* **2006**, *128*, 13806–13814.
[48] M. A. Dechantsreiter, E. Planker, B. Matha, E. Lohof, G. Holzemann, A. Jonczyk, S. L. Goodman, H. Kessler, *J. Med. Chem.* **1999**, *42*, 3033–3040.
[49] R. Haubner, D. Finsinger, H. Kessler, *Angew. Chem.* **1997**, *109*, 1440–1456; *Angew. Chem. Int. Ed. Engl.* **1997**, *36*, 1374–1389.
[50] T. Ishibashi, D. P. Bottaro, A. Chan, T. Miki, S. A. Aaronson, *Proc. Natl. Acad. Sci. USA* **1992**, *89*, 12170–12174.
[51] J. L. Todd, K. G. Tanner, J. M. Denu, *J. Biol. Chem.* **1999**, *274*, 13271–13280.
[52] A. Alonso, S. Rahmouni, S. Williams, M. van Stipdonk, L. Jaroszewski, A. Godzik, R. T. Abraham, S. P. Schoenberger, T. Mustelin, *Nat. Immunol.* **2003**, *4*, 44–48.
[53] S. Rahmouni, F. Cerignoli, A. Alonso, T. Tsutji, R. Henkens, C. J. Zhu, C. Louis-Dit-Sully, M. Moutschen, W. Jiang, T. Mustelin, *Nat. Cell Biol.* **2006**, *8*, 524–531.
[54] T. Hamaguchi, T. Sudo, H. Osada, *FEBS Lett.* **1995**, *372*, 54–58.
[55] T. Hamaguchi, A. Takahashi, T. Kagamizono, A. Manaka, M. Sato, H. Osada, *Bioorg. Med. Chem. Lett.* **2000**, *10*, 2657–2660.
[56] J. M. Denu, J. E. Dixon, *Proc. Natl. Acad. Sci. USA* **1995**, *92*, 5910–5914.
[57] Z. Shi, S. Tabassum, W. Jiang, J. H. Zhang, S. Mathur, J. H. Wu, Y. Shi, *ChemBioChem* **2007**, *8*, 2092–2099.
[58] J. M. Denu, G. C. Zhou, L. Wu, R. Zhao, J. D. Yuvaniyama, M. A. Saper, J. E. Dixon, *J. Biol. Chem.* **1995**, *270*, 3796–3803.
[59] T. P. Geladopoulos, T. G. Sotiroudis, A. E. Evangelopoulos, *Anal. Biochem.* **1991**, *192*, 112–116.
[60] T. E. Bull, *J. Magn. Reson.* **1988**, *80*, 470–481.
[61] J. W. Ponder, F. M. Richards, *J. Comput. Chem.* **1987**, *8*, 1016–1024.
[62] W. L. Jorgensen, J. Tirado-Rives, *J. Am. Chem. Soc.* **1988**, *110*, 1657–1666.
[63] W. C. Still, A. Tempczyk, R. C. Hawley, T. Hendrickson, *J. Am. Chem. Soc.* **1990**, *112*, 6127–6129.
[64] P. Huang, J. Ramphal, J. Wei, C. X. Liang, B. Jallal, G. McMahon, C. Tang, *Bioorg. Med. Chem.* **2003**, *11*, 1835–1849.

Received: April 11, 2008
Published online: September 2, 2008

